

## ABSTRACT

Title of Thesis: NEW ANTIMICROBIALS BASED ON  
SYNERGISTIC INTERACTIONS BETWEEN  
PHYSICAL AND CHEMICAL STRESSORS

Heather Leigh Dolan, Masters of Food Science,  
2017

Thesis directed by: Dr. Rohan V. Tikekar  
Department of Nutrition and Food Science

Produce microbial contamination remains a U.S. food safety concern. Chlorine is widely used to clean produce, but has limited efficacy and poses health risks. This research therefore investigates two alternative antimicrobial treatments. First, inactivation of *Listeria innocua* using a combined zinc oxide (ZnO) and low-frequency ultrasound treatment was quantified. 40 mM ZnO sonicated for 8 minute reduced *Listeria innocua* populations 100,000-fold. The mechanism appeared to be Reactive Oxygen Species-mediated, and enhanced interactions between ZnO and bacteria facilitated by lowering of ZnO nanoparticle size by sonication. Second, medium-chain fatty acid (MCFA, C6, C8, C10) and mild heat (30-50 °C) treatment against *Escherichia coli* O157:H7 was observed. The combined treatment achieved more than 100,000 fold reduction in *E. coli* in solution and no significant impairment of sensory (texture, color) qualities was observed on tomatoes. Spinach treated using this treatment showed 100-fold less bacterial cross-contamination compared to treatment with water.

NEW ANTIMICROBIALS BASED ON SYNERGISTIC INTERACTIONS BETWEEN  
PHYSICAL AND CHEMICAL STRESSORS

By

Heather Leigh Dolan

Thesis submitted to the Faculty of the Graduate School of the  
University of Maryland, College Park, in partial fulfillment  
of the requirements for the degree of  
Masters of Science  
2017

Advisory Committee:

Professor Rohan V. Tikekar, Chair  
Professor Abani K. Pradhan  
Professor Qin Wang

**© Copyright 2017**

**Heather Dolan. All rights reserved.**

## Acknowledgements

I am incredibly grateful for the opportunity to pursue a Master's in Food Science full-time at the University of Maryland over the last eighteen months. I could not have completed my thesis work without USDA funding or the support, input, and resources provided by my advisor, NFSC faculty and students, collaborators from other universities, and family.

First, I am much obliged to the USDA's National Institute of Food and Agriculture (USDA-NIFA) Program in Improving Food Quality (A1361) for providing funding via Agriculture and Food Research Initiative grant no. 2016-67017-24599.

I would next like to thank my advisor, Dr. Rohan Tikekar, for his mentorship. He provided me with a very interesting project with great relevance to the food industry. He gave me free-range in performing experiments, but also was willing to meet with me or answer emails whenever I hit a stumbling block. Further, he provided highly detailed and helpful feedback on my thesis-related writing.

I would also like to thank Dr. Tikekar's post-doctoral students, Dr. Luis Bastarrachea and Dr. Solmaz Alborzi, for their tremendous assistance in carrying out experiments. Without Dr. Bastarrachea's help, I would not have learned how to perform microbiology or have Scanning Electron Microscopy images included in my results. And without Dr. Alborzi's guidance, I would not have been able to conduct practical experiments on fresh produce.

I am also indebted to Dr. Qin Wang at the University of Maryland and her PhD student, Jinglin Zhang, for generously allowing me to use their Dynamic Light Scattering instrument to measure zinc oxide nanoparticle size. Thanks, too, to Dr. Kirk Dolan within

the Department of Food Science and Human Nutrition at Michigan State University for his guidance in kinetic modeling of bacterial inactivation.

Special mention to my fellow lab mates for keeping the lab running and letting me borrow TSA plates when I was in a fix: Solmaz Alborzi, Luis Bastarrachea, Qiao Ding, Andrea Gilbert, and Qingyang Wang.

Finally, I am always and ever grateful to my parents and brother and sister, for their constant support and for cheering me on in all my endeavors.

## Table of Contents

Acknowledgements .....	ii
List of Tables .....	vi
List of Figures.....	vii
<b>1. Introduction.....</b>	<b>1</b>
<b>1.1 Prevalence of Produce-related Foodborne Illness .....</b>	<b>1</b>
<b>1.2 Existing Sanitation Technologies for Fresh Produce and their Limitations .....</b>	<b>2</b>
<b>1.3 Novel, Alternative Sanitation Technologies for Fresh Produce.....</b>	<b>4</b>
<i>1.3.1 Ultrasound and Zinc Oxide Treatment .....</i>	<i>4</i>
<i>1.3.2 Medium Chain Fatty Acids and Heat Treatment .....</i>	<b>5</b>
<b>1.4 Research Objectives and Hypotheses.....</b>	<b>7</b>
<i>1.4.1 Ultrasound and ZnO Treatment.....</i>	<i>7</i>
<i>1.4.2 Medium Chain Fatty Acids and Heat Treatment .....</i>	<i>8</i>
<b>2. Ultrasound and Zinc Oxide.....</b>	<b>11</b>
<b>2.1 Materials and Methods.....</b>	<b>11</b>
<b>2.1.1 Microorganisms and Growth Conditions .....</b>	<b>11</b>
<b>2.1.2 Ultrasound Equipment and Parameters .....</b>	<b>11</b>
<b>2.1.3 Antimicrobial Treatments.....</b>	<b>12</b>
<b>2.1.4 L-Histidine Treatments .....</b>	<b>13</b>
<b>2.1.5 Particle Size Measurements .....</b>	<b>13</b>
<b>2.1.6 Scanning Electron Microscopy .....</b>	<b>13</b>
<b>2.1.7 Survival Curve Fitting.....</b>	<b>14</b>
<b>2.1.8 Statistical Analysis .....</b>	<b>14</b>
<b>2.2 Results and Discussion.....</b>	<b>14</b>
<b>2.2.1 Antimicrobial Effect of Combined ZnO/Ultrasound.....</b>	<b>14</b>
<b>2.2.2 L-Histidine Inhibits Antimicrobial Effect of ZnO/Ultrasound Treatment .....</b>	<b>18</b>
<b>2.2.3 Effect of Sonication on ZnO Particle Size.....</b>	<b>19</b>
<b>2.2.4 SEM Analysis .....</b>	<b>21</b>
<b>3. Heat and Medium Chain Fatty Acid.....</b>	<b>23</b>
<b>3.1 Materials and Methods.....</b>	<b>23</b>
<b>3.1.1 Microorganisms and Growth Conditions .....</b>	<b>23</b>

<b>3.1.2 Medium Chain Fatty Acid Preparation</b> .....	23
<b>3.1.3 Antimicrobial Treatments</b> .....	23
<b>3.1.4 Response Surface Analysis</b> .....	24
<b>3.1.5 Texture and Color Analyses</b> .....	24
<b>3.1.6 Spinach Cross Contamination Study</b> .....	25
<b>3.1.7 Statistical Analysis</b> .....	25
<b>3.2 Results and Discussion</b> .....	26
<b>3.2.1 Antimicrobial Effect of Combined Heat/MCFA and Response Surface Analysis</b> .....	26
<b>3.2.2 Sensory Quality of Treated Grape Tomatoes</b> .....	27
<b>3.2.3 Ability of Combined Heat/MCFA to Inhibit Spinach Cross Contamination</b> ...	30
<b>4. Conclusions and Future Studies</b> .....	31
<b>Appendix</b> .....	33
<b>References</b> .....	43

## List of Tables

<b>Table 1.</b> Characterization of ZnO nanoparticles. ....	20
<b>Table 2.</b> Characterization of ZnO nanoparticles. ....	20
<b>Table 3.</b> Inactivation of <i>E. coli</i> O157:H7 in Box-Behnken Trials. ....	26
<b>Table 4.</b> Effect Summary of Response Surface Analysis. ....	27
<b>Table 5.</b> Optimal Solution for Response Surface Analysis.....	27
<b>Table 6.</b> Hardness of control versus treated (2 min., 45 °C, in 9.8 mM octanoic acid) grape tomatoes. ....	28
<b>Table 7.</b> Color parameters for control versus treated (2 min., 45 °C, in 9.8 mM octanoic acid) grape tomatoes .....	29



## List of Figures

<b>Figure 1.</b> Ultrasound experimental set-up.....	12
<b>Figure 2.</b> Logarithmic reduction of <i>L. innocua</i> during 40 mM ZnO + ultrasound treatment. ....	16
<b>Figure 3.</b> Logarithmic reduction of <i>L. innocua</i> during 20 mM ZnO + ultrasound treatment. ....	17
<b>Figure 4.</b> Comparison in logarithmic reduction of <i>L. innocua</i> when treated simultaneously versus separately with ultrasound and 40 mM ZnO. ....	18
<b>Figure 5.</b> Attenuation of 40 mM ZnO/ultrasound/s antibacterial effect on <i>L. innocua</i> when 10 mM L-Histidine is added.....	19
<b>Figure 6.</b> Effect of sonication and L-Histidine on ZnO nanoparticle size. ....	21
<b>Figure 7.</b> SEM images of <i>L. innocua</i> in unsonicated 40 mM ZnO. ....	22
<b>Figure 8.</b> Texture profile analysis for treated (2 min., 45 °C, in 9.8 mM octanoic acid) and untreated grape tomatoes.....	28
<b>Figure 9.</b> RGB values for treated (2 min., 45 °C, in 9.8 mM octanoic acid) and untreated grape tomatoes. ....	29
<b>Figure 10.</b> Cross-contamination of spinach leaves exposed to <i>E. coli O157:H7</i> after treatment 2 min., 45 °C, in 9.8 mM octanoic acid). C: control leaf; I: inoculated leaf; CC1-CC3: cross contaminated leaves.....	30
<b>Figure 11.</b> Effect of volume sonicated on % relative fluorescence of fluorescein. ....	34
<b>Figure 12.</b> Effect of combined ZnO and sonication on % relative fluorescence of fluorescein. ....	35

<b>Figure 13.</b> Effect of increasing concentration of sonicated ZnO on % relative fluorescence of fluorescein. ....	36
<b>Figure 14.</b> Standard curve of hydrogen peroxide measurement by Amplex Red Assay. ....	37
<b>Figure 15.</b> Hydrogen peroxide generation upon 30 min. sonication of 0-1 mM ZnO. ....	37
<b>Figure 16.</b> Standard curve of hydrogen peroxide concentration by FOX Assay. ....	39
<b>Figure 17.</b> Hydrogen peroxide generated in DI water and 1 mM ZnO when sonicated 0-60 min. ....	40
<b>Figure 18.</b> Hydrogen peroxide generated in DI water and 4 mM ZnO when sonicated 0-60 min. ....	41
<b>Figure 19.</b> Hydrogen peroxide generated in DI water and 40 mM ZnO when sonicated 0-45 min. ....	42

# 1. Introduction

## 1.1 Prevalence of Produce-related Foodborne Illness

The Center for Disease Control (CDC) estimates that 1 in 6 Americans (or 48 million people) fall sick, 128,000 are hospitalized, and 3,000 die of foodborne diseases each year (CDC, 2016). In a study of foodborne outbreaks in seventeen food commodities between 1998 and 2008, the authors attributed 46% of foodborne illnesses, 38% of hospitalizations, and 23% of deaths to consumption of fresh produce. Leafy vegetables were associated with more illnesses (22%) than any other commodity examined, and were the second most frequent cause of hospitalizations (14%) (Painter et al., 2013).

Bacterial foodborne pathogens that have been linked to fresh produce disease outbreaks include *Clostridium botulinum*, *Escherichia coli* (*E. coli*) 0157:H7, *Salmonella enterica* spp., *Shigella* spp., and *Listeria monocytogenes*. Parasites tied to produce-associated illness are *Cryptosporidium* spp. and *Cyclospora* spp., while viruses prevalent on produce are Hepatitis A and Norovirus (FDA, 2001). Produce can be contaminated with microbial pathogens at any point in the food handling chain – production, harvest, processing, transport, retail, foodservice establishment, home kitchen – and is intensified by improper handling and storage prior to consumption (FDA, 2001).

Recent produce-related disease outbreaks include *Salmonella* Saintpaul contaminated jalapeño and serrano peppers and pepper products in 2008, which sickened 1,442 people in 43 states; *Salmonella* Typhimurium and *Salmonella* Newport on cantaloupe in 2012, which sickened 261 people in 24 states; and *Salmonella* Newport contamination of cucumbers in 2014, which sickened 257 people in 29 states and the

District of Columbia. The deadliest outbreak since 1990 was in 2011, when *Listeria monocytogenes*-contaminated cantaloupes resulted in 147 illnesses and 33 deaths across 28 states (CSPI, 2015).

## **1.2 Existing Sanitation Technologies for Fresh Produce and their Limitations**

Fresh and fresh-cut fruits and vegetables are disinfected during a washing step designed to remove dirt, pesticide residues, and both pathogenic and spoilage microorganisms. However, minimal processing of fresh fruits and vegetables makes it difficult to fully eliminate pathogenic organisms (FSA, 2015). Washing with chlorine-based sanitizers is almost universally used in the fresh produce industry to remove harmful bacteria and other microorganisms. Peroxyacetic acid is an attractive alternative, due to its efficacy and quick decomposition into harmless chemicals, which has been applied to fresh produce in recent years. However, chlorine-based sanitizers remain dominant due to the higher cost of peracetic acid (Lawton and Kinchla, 2015). Sodium hypochlorite, a powerful disinfectant with oxidizing properties, is most commonly used to sanitize both products and processing equipment. When sodium hypochlorite is added to water, at concentrations ranging from 50 to 200 ppm, it generates the antimicrobial agent hypochlorous acid (Artés et al., 2009). Chlorine's effectiveness against microorganisms is dependent on pH, temperature, concentration, organic matter present in the wash water, exposure time, and initial microbial load (Boyette et al., 1993).

Chlorine based sanitizers are not completely effective (Rico et al., 2007). Beuchat (1999) reported that spray treatment with 200 ppm chlorine was equally ineffective at eliminating low levels ( $10^0$  to  $10^1$  CFU/g) of *E. coli* O157:H7 on iceberg lettuce as was spraying with water. Zhang and Farber (1996) treated shredded iceberg lettuce inoculated

with 4 log(CFU/g) *Listeria monocytogenes* 10 min. with 200 ppm chlorine, resulting in only 1.3 and 1.7 log(CFU/g) reductions of *L. monocytogenes* at 4 and 22°C, respectively. Li et al. (2001) immersed cut lettuce leaves in water at 20 and 50 °C with or without addition of 20 mg/L chlorine, and found that both treatment types reduced the initial population of aerobic microorganisms by 1.73-1.96 log(CFU/g). However, overall they found the addition of chlorine had no significant effect on these reductions. Beuchat and Brackett (1990) found that typical packaging and distribution procedures – chlorine treatment, modified atmosphere packaging and shredding – did not influence or decrease growth of *L. monocytogenes* on lettuce. According to Ahvenainen (1996), chlorine compounds are not very effective at inhibiting growth of *L. monocytogenes* on shredded lettuce or Chinese cabbage, nor are they necessarily effective at reducing aerobic microbial counts in root vegetables.

Chlorine based sanitizers also pose several health risks. Wash water rapidly acquires a high organic load during produce washing, due to the introduction of soil, leaves, and other debris along with the produce. Free chlorine reacts with this organic matter, which both decreases the amount of chlorine available to kill harmful microorganisms, and results in the formation of undesirable by-products. These by-products include trihalomethanes, haloacetic acids, haloketones, and chloropicrin, all of which are potentially carcinogenic (Gil et al., 2009). While toxicity studies show that the concentration of by-products formed is negligible, the use of chlorine-based sanitizers is increasingly less popular with consumers, and has already been banned in several European countries, such as Germany, Switzerland, Denmark, and Belgium (Gil et al., 2009).

### 1.3 Novel, Alternative Sanitation Technologies for Fresh Produce

#### 1.3.1 Ultrasound and Zinc Oxide Treatment

Low-frequency (20-100 kHz) ultrasound, as an alternative antimicrobial treatment, has the advantages of being considered safe, non-toxic, and environmentally friendly (Bermúdez-Aguirre et al., 2011). The ultrasonic waves create changes in pressure, which results in cavitation bubbles that, upon bursting, kill bacteria (Piyasena et al., 2003). However, low-frequency ultrasound alone has limited application to the food industry because of time-constraints. The performance standard for food-contact surfaces is a 5-log(CFU/mL) reduction of microbial growth within 30 s (AOAC International, 2009). However bacteria, particularly spores, are very resistant and would require hours of sonication to be inactivated (Sala et al., 1995). In one study, complete sterilization of an *E. coli* film grown for 14 h was achieved after 6 h of exposure to low-frequency ultrasound (Johnson et al., 2012). In another study, low-frequency ultrasound alone was found to kill less than 1 log (90%) of the foodborne pathogens *E. coli*, *Staphylococcus aureus*, *Pseudomonas aeruginosa*, and *Bacillus subtilis* (Scherba et al., 1991). Ultrasound in combination with pressure (Mañas et al., 2000) and/or heat (Ordoñez et al., 1987) has been shown to enhance microbial inactivation (Piyasena et al., 2003). Studies have been done examining the combined effect of ultrasound and heat/chemicals on alfalfa seeds (Scouten and Beuchat, 2002), and of ultrasound and heat/pressure on fruit and vegetable juices (Kuldiloke, 2002). One combination that has not been explored is ultrasound treatment of microorganisms in the presence of sonochemicals, such as zinc oxide (ZnO) and titanium dioxide (TiO<sub>2</sub>). ZnO is an inorganic compound with known antibacterial properties. Brayner et al. (2006) observed that interactions between ZnO nanoparticles

and *E. coli* resulted in cell wall disorganization and internalization of nanoparticles into cells. In a study comparing antibacterial ability of six metal oxide nanoparticle types (MgO, TiO<sub>2</sub>, Al<sub>2</sub>O<sub>3</sub>, CuO, CeO<sub>2</sub>, and ZnO), ZnO had significantly higher antibacterial activity against *Staphylococcus aureus* than did any of the other five metal oxides (Jones et al., 2008). A number of studies have shown that ZnO's antibacterial efficacy increases with increasing concentration (Jalal et al., 2010; Emami-Karvani and Chehrazi, 2011), and with decreasing nanoparticle size (Padmavathy and Vijayaraghavan, 2008; Raghupathi et al., 2011). ZnO is generally recognized as safe (GRAS) by the Food and Drug Administration, and is currently used as a food additive. ZnO nanoparticles have known antibacterial ability, and have already been incorporated into food packaging material to improve its antibacterial activity (Espitia et al., 2012). However, little is known about its synergistic interaction with ultrasound to enhance microbial inactivation.

### *1.3.2 Medium Chain Fatty Acids and Heat Treatment*

Fatty acids (FAs) are ubiquitous molecules typically bound to glycerol, sugars, or phosphate head groups to form lipids. When FAs are released from lipids, they form free fatty acids (FFAs), which exhibit an array of powerful biological activities (Desbois and Smith, 2010). The antibacterial effects of FFAs have been well-studied. In humans, FFAs including dodecanoic acid (C12:O), tetradecanoic acid (C14:O), and hexadecanoic acid (C16:O), act as antimicrobial agents within skin lipids (Takigawa et al. 2005; Georgel et al. 2005; Kenny et al. 2009). Further, medium- and long-chain saturated FFAs inhibit the urinary tract pathogen *Proteus mirabilis* (Liaw et al., 2004). In microorganisms such as microalgae, release of FFAs within the cell membrane and energy storage structures

during cellular disintegration may serve as a 'population level' defense against pathogenic bacteria and viruses (Desbois and Smith, 2010).

FFAs are an attractive food antimicrobial because they are natural, Generally Recognized as SAFE (GRAS), exhibit a broad spectrum of activity, and are non-specific in their mode of action. Further, the FDA identifies octanoic and decanoic acids as safe for direct addition to food for human consumption as long as they are free of chick-edema factor and not made up of more than 2% unsaponifiable matter (FDA, 2016).

Now that the European Union has banned use of antibiotics in livestock foodstuffs, FFAs could serve as a potential alternative antimicrobial (Desbois and Smith, 2010). To enhance FFAs antibacterial effect, their use in combination with heat has been suggested as a hurdle technology for food preservation (Mvou et al, 2010). The inhibitory effect of heat-treated FFAs on different bacterial species is well-documented. FFAs' antibacterial mechanism has not been fully characterized. However, it appears that FFAs target the bacterial cell membrane and essential processes occurring at the cell membrane. Due to their amphipathic structure, FFAs can act as detergents at higher concentrations, thereby solubilizing the cell membrane (Desbois and Smith, 2010). FFAs can also interfere with the electron transport chain and disrupt oxidative phosphorylation (Sheu and Freese, 1972; Galbraith and Miller, 1973; Miller et al., 1977; Boyaval et al., 1995; Wojtczak and Wieckowski, 1999). It's also possible that FFAs kill bacteria via cell lysis, inhibiting enzyme activity, preventing nutrient uptake, or generating toxic products (Desbois and Smith, 2010). Tsuchido and Takano (1998) found that growth of *E. coli* K-12 cells heat-treated at 55 °C for 15 s was more significantly delayed by the MCFAs octanoic and decanoic acid than by butanoic, hexanoic, or dodecanoic acids. Jang and



Rhee (2009) determined that reconstituted infant formula treated with 10, 20, or 30 mM octanoic acid at 45, 50, or 55 °C had more rapid *Cronobacter* spp. reductions with increasing octanoic acid concentration and temperature. At 55 °C, they reported *Cronobacter* spp. reductions of 2.25, 4.81, and 6.30 log(CFU/mL) after 10 min. for 5, 10, and 20 mM octanoic acid treatments, respectively, versus a 4.14 log(CFU/mL) reduction after 60 min. for the control, heat treated infant formula alone. Marounek et al. (2012) similarly reported that 30 min. treatment with 13.9 mM octanoic acid at 37 °C reduced *Cronobacter sakazakii* by 5.40 log(CFU/mL), and reduced *Cronobacter malonaticus* to below the limits of detection in comparison to the control.

Within the food industry, short chain fatty acids have been incorporated into sprays for sanitizing meat, and have also been applied as fungistats in animal feeds. Dickson (1992) observed a 1 log reduction in *Salmonella* Typhimurium on beef fat tissue after treatment with 2% acetic acid. Paster (1979) found that propionic acid is a better inhibitor of mold in poultry feed under summer conditions than is calcium propionate. However, to the best of our knowledge no practical studies have been done examining the effect of heated MCFAs on fresh produce.

## **1.4 Research Objectives and Hypotheses**

### *1.4.1 Ultrasound and ZnO Treatment*

The objectives of the first study were to determine the effect of ultrasound in combination with ZnO in the inactivation of *Listeria innocua* (*L. innocua*), and to understand the mechanism(s) by which these two treatments kill bacteria. *L. innocua* is an excellent non-pathogenic surrogate for the foodborne pathogen *Listeria*

*monocytogenes* because it has nearly identical physiological characteristics and is even more resistant to thermal processing (Friedly et al., 2008).

Low-frequency ultrasound's primary mechanism of action is its cavitation effect. When a liquid is sonicated, the acoustic vibrations are converted into microscopic gas bubbles. Cycles of low and high acoustic pressure in the incident acoustic wave cause these bubbles to expand and shrink. Beyond their tensile strength, cavitation bubbles violently collapse and produce localized areas of extreme pressure (1000 atm) and temperature (5000 K). These high levels of temperature and pressure can then fragment water and other molecules into free radicals (Erriu et al., 2013). These free radicals, or ROS, include hydroxyl ions, peroxide, superoxide, and singlet oxygen. ROS can cause damage to bacteria cell membrane, protein, and DNA structures, ultimately resulting in cell death (Villamiel et al., 2015). In addition, other research groups have reported that ZnO nanoparticles are capable of producing ROS (Lipovsky et al., 2011; Sawai et al., 1998). Therefore, we hypothesized that the bactericidal mechanism of sonicated ZnO involves ROS generation.

The physical structure of a nanoparticle affects the way in which it interacts with and penetrates bacteria. Previous studies have shown that ultrasound breaks apart agglomerates of ZnO nanoparticles, resulting in increased interaction with bacteria (Seil and Webster, 2012), and that smaller particle size corresponds to greater efficacy in inhibiting bacterial growth (Seil and Webster, 2012; Lipovsky et al, 2011). Thus, we hypothesized that the bactericidal mechanism of sonicated ZnO also relates to the enhanced ability of ZnO to interact with and damage bacteria post-sonication.

#### *1.4.2 Medium Chain Fatty Acids and Heat Treatment*

The objectives of the second study were to determine optimal conditions for inactivation of *E. coli* O157:H7 with mild heating and MCFA, and to apply these conditions to actual produce. *E. coli* O157:H7 was used in this study rather than *L. innocua* because it has been shown to be less heat resistant in numerous studies. Murphy et al. (2004) found that for a cocktail of *L. monocytogenes*, *Salmonella enterica* spp., and *E. coli* O157:H7 in ground beef/turkey heat resistance of *L. monocytogenes* at 55-70 °C was 45-81% higher than that of *E. coli* O157:H7. Sharma et al. (2005) reported that *L. monocytogenes* was more heat resistant than *E. coli* O157:H7 when heated at 57 °C in cantaloupe juice. In addition, previous studies demonstrating the antibacterial effect of fatty acids have all been done on gram negative bacteria, including *E. coli* (Hassinen et al., 1951), *Salmonella* (Van Immerseel et al., 2004), and *Campylobacter jejuni* (Thormar et al., 2006).

First, Box-Behnken design of experiments was performed to identify optimal MCFA type (hexanoic, octanoic, or decanoic), MCFA concentration (0, 5, or 10 mM) and temperature (30, 40, or 50 °C) for inactivating *E. coli* O157:H7. A non-pathogenic strain of *E. coli* O157:H7 with the shiga toxins removed, ATCC 700728, was used because it has been shown to have similar survival behavior to non-pathogenic *E. coli* O157:H7 in numerous practical studies performed on lettuce (Gurtler et al., 2010; Kim et al., 2009). Optimal treatment conditions were then applied to both a spinach leaf inoculated with 6 log(CFU/mL) *E. coli* O157:H7 and three non-inoculated spinach leaves to determine efficacy in preventing cross contamination.

Existing studies on the effect of heat treated fatty acids on bacteria suggest that 10 min. treatment with octanoic acid results in antimicrobial activity against *Cronobacter*

spp. at concentrations as low as 20 mM and temperatures as low as 45 °C (Jang and Rhee, 2009), while 30 min. treatment achieves an antimicrobial effect against *Cronobacter sakazakii* and *Cronobacter malonaticus* at 13.9 mM and 37 °C (Marounek et al, 2012). Other studies have not shown hexanoic acid to be an effective antimicrobial against *E. coli* K12 cells, but have suggested that decanoic acid is (Tsuchido and Takano, 1998). Based on the results of these studies, we hypothesized that the antimicrobial effect will be most significant at the highest temperature (50 °C) and concentration (10 mM), and for the longest chain fatty acid (decanoic). Considering the shorter treatment time (2 min.) and lower temperature range (30-50 °C) we hypothesize a less marked antimicrobial effect for all of our treatments.

## **2. Ultrasound and Zinc Oxide**

### **2.1 Materials and Methods**

#### **2.1.1 Microorganisms and Growth Conditions**

*L. innocua* Clip11262 was obtained from Dr. Robert Buchanan, Department of Nutrition and Food Science at the University of Maryland-College Park. Bacterial suspensions were prepared as follows: stock cultures were kept in Tryptic Soy Broth (TSB, Difco, Becton Dickinson, Sparks, MD), containing 25% glycerol at -80 °C. A loopful of stock culture was streaked onto tryptic soy agar (TSA, Difco, Becton Dickinson, Sparks, MD) and incubated at 37 °C for 24 h. An individual colony was taken from the inoculated TSA and transferred to 9 mL of sterile TSB. The broth was subsequently incubated overnight at 37 °C for 12-14 h, and streaked onto new TSA plates, which were incubated for 24 h at 37 °C. TSA plates were refrigerated and kept for experiments up to three weeks.

An individual colony of *L. innocua* was taken from the TSA plates, transferred to 9 mL of sterile TSB, and incubated overnight at 37 °C. After 14-15 h incubation, the cells were diluted 100-fold in sterile TSB, and incubated at the same temperature an additional 5 hours, until the middle of the exponential phase. After this second incubation period, the cells were subjected to the antimicrobial treatments described in section 2.1.3.

#### **2.1.2 Ultrasound Equipment and Parameters**

The sonic dismembrator is a model FB505 (Fisher Scientific, Pittsburgh, PA), with a maximum power of 500 W and a frequency of 20 kHz. The probe has a replaceable tip (12.7 mm diameter), and experiments were performed at 50% amplitude, or 120 µm (Qsonica, LLC., Newtown, CT), and at a wattage of 43–45 W. The probe was immersed in

bacterial suspensions to a depth of 1 cm. 50 mL bacterial suspensions were placed in a 100 mL jacketed glass beaker (Kimble Chase, Vineland, NJ) and stirred continuously via a magnetic rod (Figure 1). Both probe and suspensions were housed within a sound enclosure chamber. For all treatments, the bacterial suspensions' temperature was maintained at  $22.0 \pm 1.0$  °C using a refrigerated bath.

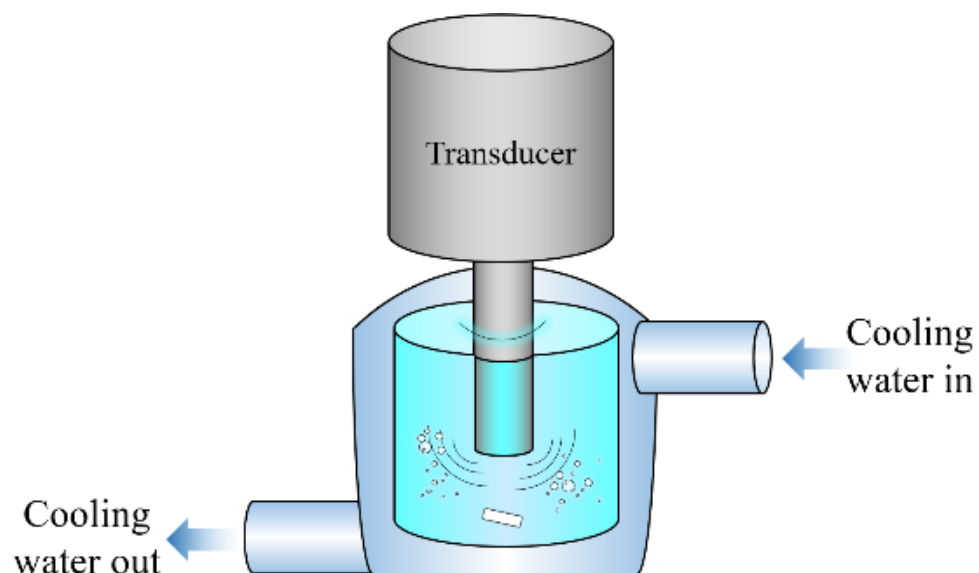


**Figure 1.** Ultrasound experimental set-up.

### 2.1.3 Antimicrobial Treatments

Bacterial suspensions of 6 log (CFU/mL) *L. innocua* in 40 mM ZnO were prepared by transferring mid-exponential phase *L. innocua* to 50 mL of 40 mM ZnO in DI water. The ZnO-bacteria suspension was subsequently sonicated for 0, 4, 8, and 12 min. in triplicate. Similarly, bacterial suspensions were prepared in 20 mM ZnO, and subsequently sonicated in triplicate, but at different time intervals each experiment run, for 0-30 min. After treatment, bacterial suspensions were serially diluted in 0.1% peptone

water, plated on TSB, and plate-counted after 24 h incubation at 37 °C. Controls consisted of 6 log(CFU/mL) *L. innocua* in 40 mM without sonication at 0 min. and at last kinetic timepoint, (12 min.), as well as 6 log(CFU/mL) *L. innocua* sonicated without addition of 40 mM ZnO at 0 and 12 min.

#### **2.1.4 L-Histidine Treatments**

To determine whether bacterial inactivation was Reactive Oxygen Species (ROS) mediated, 10 mM histidine was added to 6 log(CFU/mL) *L. innocua* in 40 mM ZnO (total volume: 50 mL), prior to sonication for 0, 4, 8, and 12 min. Histidine's inhibition of the combined ZnO and sonication treatment's antimicrobial effect was enumerated via plating serial dilutions of bacterial suspensions in 0.1% peptone water, and plate-counting after 24 h incubation at 37 °C.

#### **2.1.5 Particle Size Measurements**

ZnO nanoparticle size measurements were taken to determine the effect of sonication, using a BI-200 SM Goniometer Version 2 Dynamic Light Scattering instrument (Brookhaven Instruments, Holtsville, NY), equipped with a 35 mW He-Ne laser. The following parameters were adopted: detection wavelength of 637 nm and scattering angle of 90°. 2 mL samples of sterile 40 mM ZnO sonicated for 0, 4, 8, and 12 min. were analyzed, as well as 2 mL samples of 40 mM ZnO and 10 mM histidine sonicated for the same time intervals.

#### **2.1.6 Scanning Electron Microscopy**

Control samples (20 mL, ~ 7 log(CFU/mL)) of 40 mM ZnO were filtered through a 0.2 µm pore filter (25 mm, EMD Millipore Co., Billerica, MA). The filter was then

immersed in 10 mL of 0.25% Glutaraldehyde in DI water (Sigma-Aldrich, St. Louis, MO) for 1 h. The filter was next rinsed three times in DI water, then immersed in 10 mL aqueous solutions with increasing concentration of ethanol (v/v: 10%, 25%, 50%, 75%, 90% and 100%). The filter was kept in anhydrous calcium sulfate until analysis. Finally, the filter was sputter-coated with gold for 1 min., after which SEM analysis was performed with a TESCAN XEIA FEG Scanning Electron Microscope (TESCAN, Ltd., Brno, Czech Republic) at 5 kV (Sousa et al., 2015; Kihm et al., 1994).

### 2.1.7 Survival Curve Fitting

The survival curves were fitted into a first-order kinetic model to model inactivation:

$$\log N(t) = \log N_0 - kt \quad (1)$$

where  $N(t)$  is the concentration of bacteria at time  $t$ ,  $N_0$  is the concentration of the untreated population, and  $k$  is the inactivation rate constant (Xiong et al., 1999).

### 2.1.8 Statistical Analysis

Differences between sample means for bacteria treated with combined ultrasound and ZnO versus bacteria treated with either treatment separately were analyzed using one-way ANOVA and Tukey's HSD test. Differences in nanoparticle size for ZnO nanoparticles versus ZnO in L-Histidine were analyzed using a two-tailed t-test.

## 2.2 Results and Discussion

### 2.2.1 Antimicrobial Effect of Combined ZnO/Ultrasound

The effects of different sanitizing treatments on the growth of *L. innocua* after 24 h incubation at 37 °C are shown in Figs. 2-3. As shown in Figure 2, the combined 40 mM ZnO and sonication treatment achieved a > 5 log reduction in *L. innocua* within 8 min.



According to one-way ANOVA, treatment type (US/ZnO, US, ZnO) after 8 min. had a significant effect on bacterial reduction at the  $p < 0.05$  level [ $F(2, 6) = 5043.14$ ,  $p = <0.0001$ ]. Post hoc comparisons using the Tukey HSD test indicated that the mean bacterial reduction due to combined treatment with US/ZnO ( $M = -5.00$ ,  $SD = 0.00$ ), was significantly different from the two control treatments, US alone ( $M = -0.29$ ,  $SD = 0.09$ ) and ZnO ( $M = 0.04$ ,  $SD = 0.07$ ) alone.

This reduction in *L. innocua* is significantly higher than the reduction after either ZnO or ultrasound alone after 8 min. The  $k$  value, 0.63, indicates that after a treatment time of  $t = 1/k$ , or 1.6 min, 90% of the *L. innocua* population is killed (Casolari, 1988). In comparison, incubation for 4-5 h with a much higher concentration (~184 mM) of ZnO nanoparticles alone is required to induce any antibacterial effect (Wahab et al, 2010). Jin et al. (2009) found that ZnO nanoparticles at a concentration of 122.8 mM reduced *L. monocytogenes* growth by only ~1 log after 8 h. Ferrante et al. (2007) observed a ~2 log reduction in *L. monocytogenes* in orange juice subjected to low-frequency ultrasound alone.

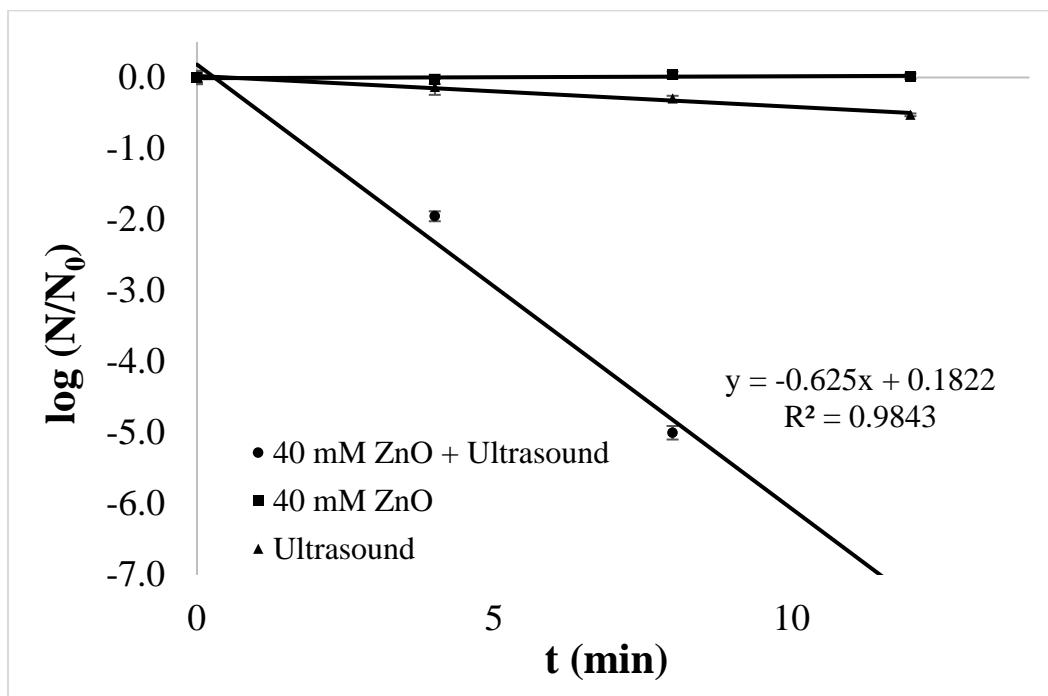


**Figure 2.** Logarithmic reduction of *L. innocua* during 40 mM ZnO + ultrasound treatment.

Figure 3 demonstrates the antimicrobial effect's concentration dependency, as only a ~3 log reduction is achieved after 20 min. of a combined US and 20 mM ZnO, compared to > 5-log reduction within 8 min. for a 40 mM ZnO treatment. The inactivation data in Figure 3 was also fitted into first order kinetics. The  $k$  value, 0.17, indicates that 90% of the *L. innocua* population is killed in 5.9 min.

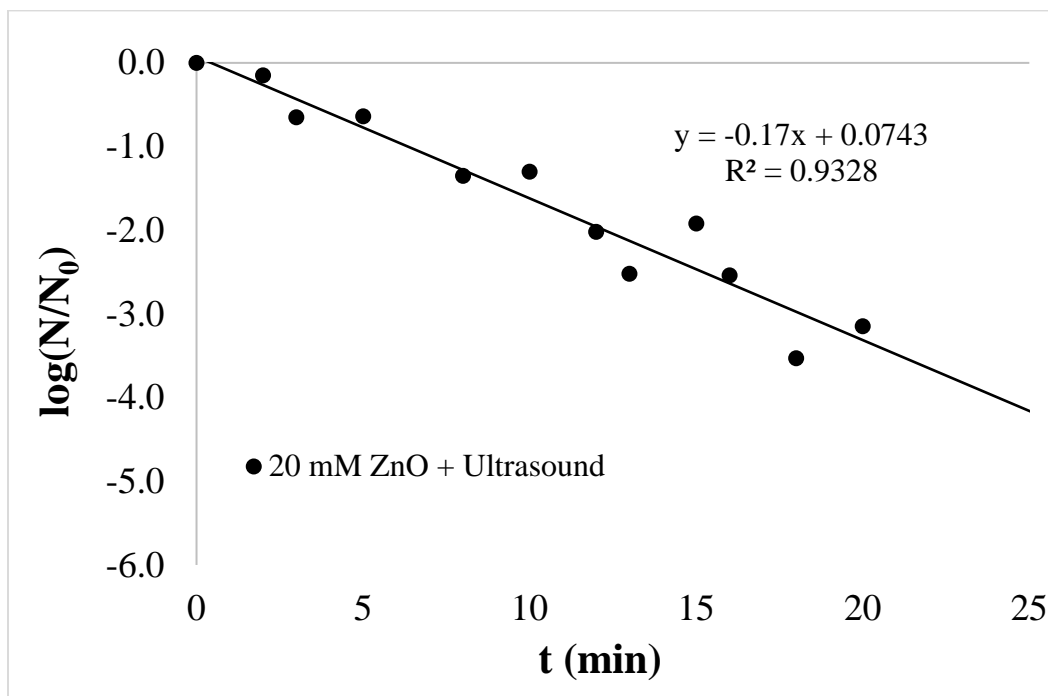


**Figure 3.** Logarithmic reduction of *L. innocua* during 20 mM ZnO + ultrasound treatment.

To demonstrate that the effect of ultrasound and ZnO is synergistic and not additive, we performed a sequential treatment where *L. innocua* were first exposed to ultrasound alone for 12 min., followed by treatment with ZnO alone for 12 min. (Figure 4). One-way ANOVA was performed to compare the endpoint of the additive treatment (at t = 24 min.) to the combined treatment and two controls (at t = 8 min.). According to this analysis, there was a significant difference in bacterial reduction at the  $p < 0.05$  level between the four treatments [ $F(3, 7) = 3367.75$ ,  $p = <0.0001$ ]. Post hoc comparisons using the Tukey HSD test indicated that the mean bacterial reduction due to the additive treatment ( $M = -1.21$ ,  $SD = 0.06$ ), was significantly different from the mean bacterial reduction for 8 min. combined treatment ( $M = -5.00$ ,  $SD = 0.00$ ). *L. innocua* first sonicated for 12 min., and subsequently immersed in 40 mM ZnO for 12 min. experienced a  $\sim 1$  log reduction, which is comparable to the bacterial reduction when *L.*

*innocua* is sonicated for 12 min. without 40 mM ZnO. The lack of further bacterial reduction after subsequent exposure to ZnO after sonication suggests that ZnO can only enhance the antibacterial effect when sonicated.

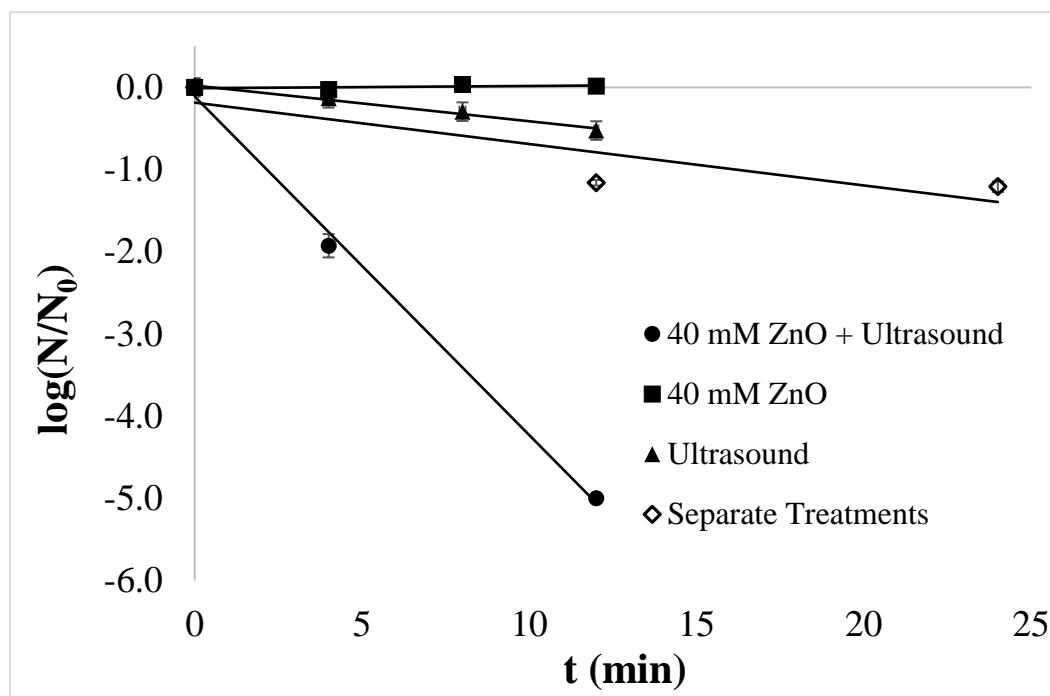


**Figure 4.** Comparison in logarithmic reduction of *L. innocua* when treated simultaneously versus separately with ultrasound and 40 mM ZnO.

### 2.2.2 L-Histidine Inhibits Antimicrobial Effect of ZnO/Ultrasound Treatment

We evaluated the antimicrobial effect of the combined treatment in the presence of histidine, a known scavenger of hydroxyl radicals and singlet oxygen (Lipovsky et al., 2011). Figure 5 below shows that in the presence of histidine, only a ~1 log reduction in *L. innocua* occurs after 8 min. sonication, compared to a >5 log reduction in the absence of histidine. This attenuation of ZnO and ultrasound's antibacterial effect strongly suggests that ROS, specifically hydroxyl radicals and singlet oxygen, contribute to the combined treatment's bactericidal mechanism.

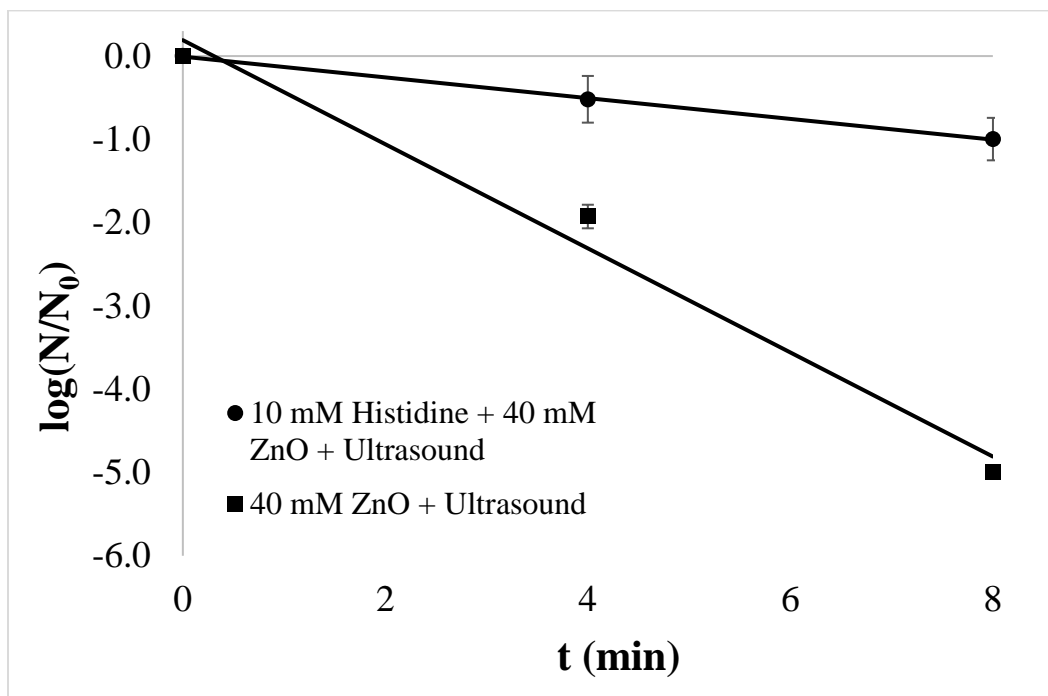


**Figure 5.** Attenuation of 40 mM ZnO/ultrasound's antibacterial effect on *L. innocua* when 10 mM L-Histidine is added.

### 2.2.3 Effect of Sonication on ZnO Particle Size

Table 1 summarizes the characterization of ZnO particles before and after treatment with ultrasound, including particle size and polydispersity (PDI). Particle size of ZnO nanoparticles (40 mM in DI water) without sonication is approximately 250 nm. ZnO nanoparticle size decreased to ~115 after 4 min. sonication, and remained at that size after further sonication for 8 and 12 min. Seil and Webster (2012) suggest that sonication disperses both nanoparticle agglomerates and bacteria colony-forming units, making it easier for nanoparticles to penetrate bacteria cell membranes. The decrease in ZnO nanoparticle size indicates a physical aspect of its antibacterial mechanism.

**Table 1.** Characterization of ZnO nanoparticles

Sonication (min.)	Particle size (nm)	PDI
0	252.5 ± 99.3	0.32
4	114.2 ± 89.9	0.29
8	104.9 ± 57.4	0.31
12	106.2 ± 44.7	0.30

To rule out the possibility of histidine having a physical effect on ZnO nanoparticle size, the same measurements were taken for ZnO (40 mM DI water) with addition of 10 mM histidine. Table 2 demonstrates that histidine did not significantly effect, at the  $p < 0.05$  level, ZnO nanoparticle size at t 0 ( $t(334) = 1.55$ ,  $p\text{-value} = 0.121$ ).

**Table 2.** Characterization of ZnO nanoparticles in presence of 10 mM L-Histidine

Sonication (min.)	Particle size (nm)	PDI
0	299.4 ± 238.2	0.33
4	140.7 ± 135.6	0.28
8	90.5 ± 106.6	0.32

Figure 6 shows a clear decrease in ZnO nanoparticle size range after sonication for 8 m. There is considerable overlap between the sonicated ZnO and sonicated ZnO in the presence of histidine nanoparticle size distributions.

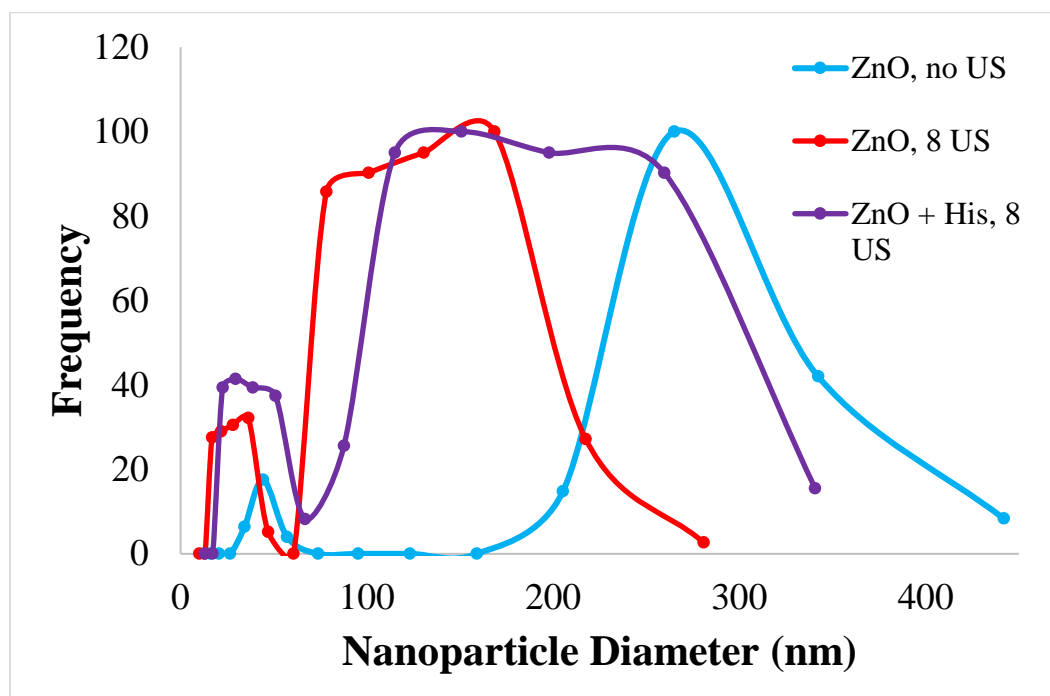


**Figure 6.** Effect of sonication and L-Histidine on ZnO nanoparticle size.

#### 2.2.4 SEM Analysis

Figure 7 shows *L. innocua* and ZnO nanoparticles observed by SEM. The *L. innocua* in each of a, b, and c was identically treated with 40 mM ZnO and no ultrasound. It appears that ZnO is associated with the bacteria, as clusters of ZnO nanoparticles are aggregated close to the bacterium in each image. Direct contact of ZnO-nanoparticles with bacterial cell walls has been suggested in literature as a potential toxicity mechanism. Specifically, Brayner et al. (2006) reported damage and disorganization in the cell wall of *E. coli* after exposure to 0.1-10.0 mM ZnO nanoparticles. Zhang et al. (2006) observed damage and breakdown of *E. coli* cell membranes exposed to 2.46 mM

ZnO. Cell wall damage suggests that ZnO can weaken and eventually permeate bacterial cell walls, leading to cell death. The association of ZnO with *L. innocua* shown in Figure 7 complements the decrease in ZnO nanoparticle size after sonication shown in Table 1. It is likely that during sonication, aggregated ZnO nanoparticles are broken apart and therefore more easily permeate through *L. innocua* cell walls.

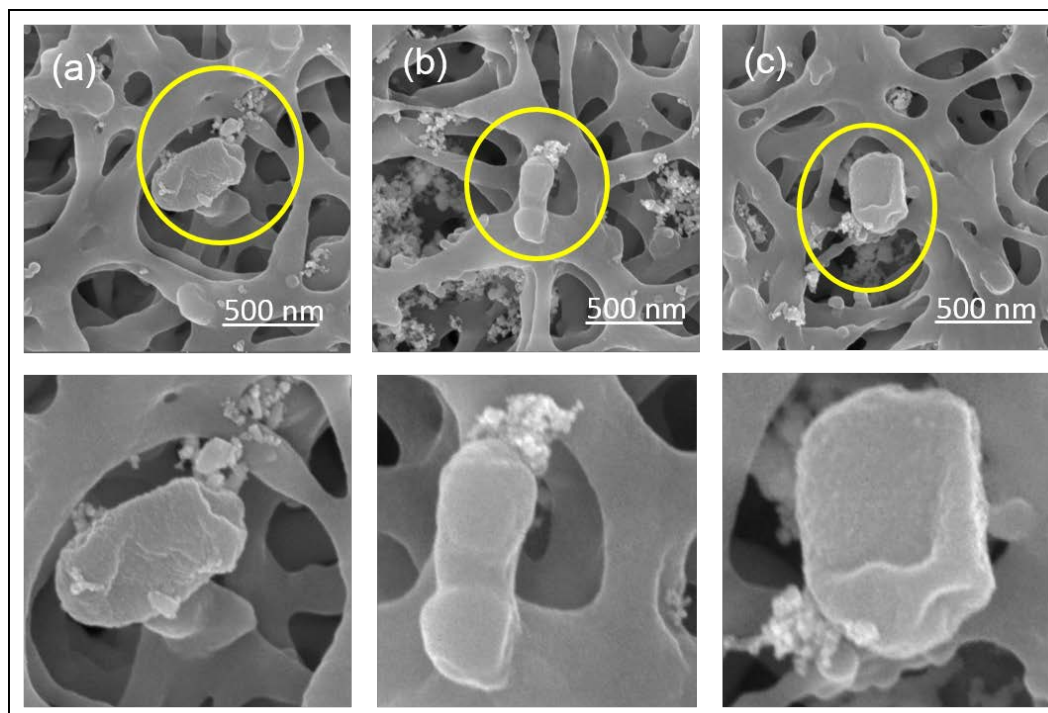


**Figure 7.** SEM images of *L. innocua* in unsonicated 40 mM ZnO.



### **3. Heat and Medium Chain Fatty Acid**

#### **3.1 Materials and Methods**

##### **3.1.1 Microorganisms and Growth Conditions**

*E.coli* O157:H7 ATCC 700728 was provided by Dr. N. Nitin, Department of Food Science and Technology at UC Davis. Bacterial suspensions were prepared and streaked onto TSA plates as described in Section 2.1.1. An individual colony of *E. coli* O157:H7 was taken from the TSA plates, transferred to 9 mL of sterile TSB, and incubated at 37 °C for 20 h, until they reached the stationary phase. The cells were then diluted 100-fold in sterile deionized (DI) water, and next subjected to the antimicrobial treatments described in section 3.1.2.

##### **3.1.2 Medium Chain Fatty Acid Preparation**

Fatty acid (hexanoic, octanoic, decanoic) was brought to 10 mL in 100% ethanol at different concentrations (0, 5, 10 mM). Hexanoic and octanoic acid are liquid, while decanoic acid is a solid; all three MCFAs are soluble in ethanol. Fatty acid solutions were subsequently filtered through a 0.2 µm pore filter (25 mm, Fisher Scientific, Pittsburgh, PA).

##### **3.1.3 Antimicrobial Treatments**

Bacterial suspensions of 6 log (CFU/mL) *E. coli* O157:H7 were prepared by first transferring stationary phase *E. coli* O157:H7 to 9 mL of pre-heated, acidic (pH ~4.5) DI water. Acidified DI water was prepared by adding 5-10 µL of 0.2 M hydrochloric acid to ~25 mL sterile DI water, then adding additional DI water until the pH reached ~4.5. The final solution was filtered through a 0.2 µm pore filter (25 mm, Fisher Scientific,

Pittsburgh, PA). Hexanoic, octanoic, or decanoic acid was next added to the bacterial suspension to a final concentration of 0, 5, or 10 mM. The final solution was then placed in a water bath at 30, 40, or 50 °C for 2 min. For a given temperature set point, the corresponding experiments were performed on the same day. After treatment, bacterial suspensions were serially diluted in 0.1% peptone water, plated on TSB, and plate-counted after 24 h incubation at 37 °C. Controls consisted of 6 log(CFU/mL) *E. coli* O157:H7 in pre-heated acidified water without addition of MCFA.

### **3.1.4 Response Surface Analysis**

To evaluate the effect of fatty acid chain length (C6, C8, C10), concentration of fatty acid (0, 5, 10 mM) and temperature (30, 40, 50 °C) on microbial inactivation, we chose a Box Behnken design for 3 variables at 3 levels. A response surface analysis was performed using JMP software. Fit model analysis of data from the Box-Behnken experiments output parameter estimates for all response surface and crossed effects in the model.

### **3.1.5 Texture and Color Analyses**

A TA-XT2i texture analyzer (Texture Technology Corp., Scarsdale, NY) was used to evaluate changes in texture for treated versus untreated grape tomatoes. Analysis was done immediately after 2 min. heat treatment at 45 °C in 9.8 mM octanoic acid. These conditions were chosen based on the optimization results from Box-Behnken design. Grape tomatoes were purchased from a major grocery store chain the day before analysis, refrigerated overnight, and kept at room temperature the day of the experiment. Samples were placed onto the press holder, and a 5 mm probe (TA-55) was moved down at 1

mm/sec. Maximum force was determined using Texture Exponent software (Stable Micro Systems, Godalming, Surrey, UK). Experiments on both control and treated samples were performed in triplicate on different grape tomatoes.

Color for treated versus untreated grape tomatoes was measured using a ColorFlex EZ spectrophotometer (HunterLab, Reston, VA). L\*, a\*, and b\* values, which indicate color lightness, redness, and yellowness, respectively, were assessed in triplicate for both control and treated grape tomatoes.

### **3.1.6 Spinach Cross Contamination Study**

Organic spinach leaves were washed in DI water and subsequently dried. A single spinach leaf was inoculated with 6 log (CFU/mL) stationary phase *E. coli* O157:H7, and placed in a stomacher bag with three non-inoculated spinach leaves. The four spinach leaves were then treated with 9.8 mM octanoic acid in acidified (pH < 4.5) DI water, and continually shaken for 2 min. in a 45 °C hot water bath. After treatment, spinach leaves were separated into individual stomacher bags, to which 0.1% peptone water was added, and homogenized for 5 min. using a stomacher (80 BA 7020 Stomacher Lab Blender, Seward, Worthing, UK). Bacterial suspensions within each stomacher bag were serially diluted in 0.1% peptone water, plated on EMB, and plate-counted after 24 h incubation at 37 °C. Spinach leaves treated with DI water served as the control. For both treated and control spinach leaves, a fifth untreated spinach leaf was inoculated with 6 log(CFU/mL) *E. coli* O157:H7.

### **3.1.7 Statistical Analysis**

Differences between mean Lab and hardness values for grape tomatoes treated with heat and octanoic acid versus untreated grape tomatoes were analyzed using a two-tailed t-test.

### 3.2 Results and Discussion

#### 3.2.1 Antimicrobial Effect of Combined Heat/MCFA and Response Surface Analysis

The bacterial inactivation for each Box-Behnken trial is shown in Table 3. Hexanoic acid has no antibacterial effect at any concentration or temperature. Octanoic acid inactivates *E. coli* O157:H7 to below the limit of detection at 5 and 10 mM concentration and at every temperature (30, 40, 50 °C). Decanoic acid demonstrates an antibacterial effect at 10 mM at every temperature, but is not as effective at 5 mM, only showing an antibacterial effect at 50 °C (40 °C not tested).

**Table 3.** Inactivation of *E. coli* O157:H7 in Box-Behnken Trials

Experimental Run	Bacteria Remaining (Log (CFU/mL))
40 °C – 5 mM – C8	<1
30 °C – 10 mM – C8	<1
40 °C – 10 mM – C10	<1
40 °C – 5 mM – C8	<1
40 °C – 5 mM – C8	<1
30 °C – 0 mM – C8	6.30
40 °C – 0 mM – C8	6.31
30 °C – 5 mM – C10	5.19
30 °C – 5 mM – C6	6.24
50 °C – 10 mM – C8	<1
50 °C – 5 mM – C6	6.17
50 °C – 0 mM – C8	6.21
50 °C – 5 mM – C10	<1
40 °C – 0 mM – C6	6.27
40 °C – 10 mM – C6	6.28

The response surface analysis is shown in Tables 4 and 5. Table 4, the effect summary, ranks the influence of each factor on the optimal solution. Concentration is the most important and temperature the least, while relationships between different factors have a minimal effect. Table 5 provides the response surface analysis solution, yielding: 45 °C, 9.8 mM, and 9.3-carbon chain length. Since a chain number of 9.3 is physically impossible, a choice must be made between chain lengths of 8 and 10. Overall, octanoic acid outperformed decanoic acid, and therefore for the applied experiment, optimal treatment conditions were: 45 °C, 9.8 mM, and 8-carbon chain length.

**Table 4.** Effect Summary for Response Surface Analysis

Source	Logworth	P Value
Concentration (0, 10)	2.475	0.00335
Chain Length*Chain Length	2.191	0.00644
Chain Length (6, 10)	1.898	0.01264
Concentration*Concentration	1.343	0.04538
Chain Length*Concentration	1.261	0.05488
Temperature*Temperature	1.038	0.09167
Temperature*Chain Length	0.954	0.11126
Temperature (30,50)	0.680	0.20885
Temperature*Concentration	0.014	0.96798

**Table 5.** Optimal Solution for Response Surface Analysis

Variable	Critical Value
Temperature (30, 50)	45.153
Chain Length (6, 10)	9.300
Concentration (0, 10)	9.807

### 3.2.2 Sensory Quality of Treated Grape Tomatoes

The results of texture analysis (Table 6) indicate no significant change at the  $p < 0.05$  level in the hardness values for treated grape tomatoes ( $t(2) = 1.30$ ,  $p\text{-value} = 0.324$ ) after washing the tomatoes with the optimized treatment.

**Table 6.** Hardness of control versus treated (2 min., 45 °C, in 9.8 mM octanoic acid) grape tomatoes

Hardness (kg)	
Control	Treated
$0.96 \pm 0.37$	$0.67 \pm 0.08$

Figure 8 shows force versus time plots for both untreated and treated grape tomatoes based on single replicate data. Tomato hardness is the peak force during compression, and is nearly indistinguishable on the graph for untreated versus treated samples.

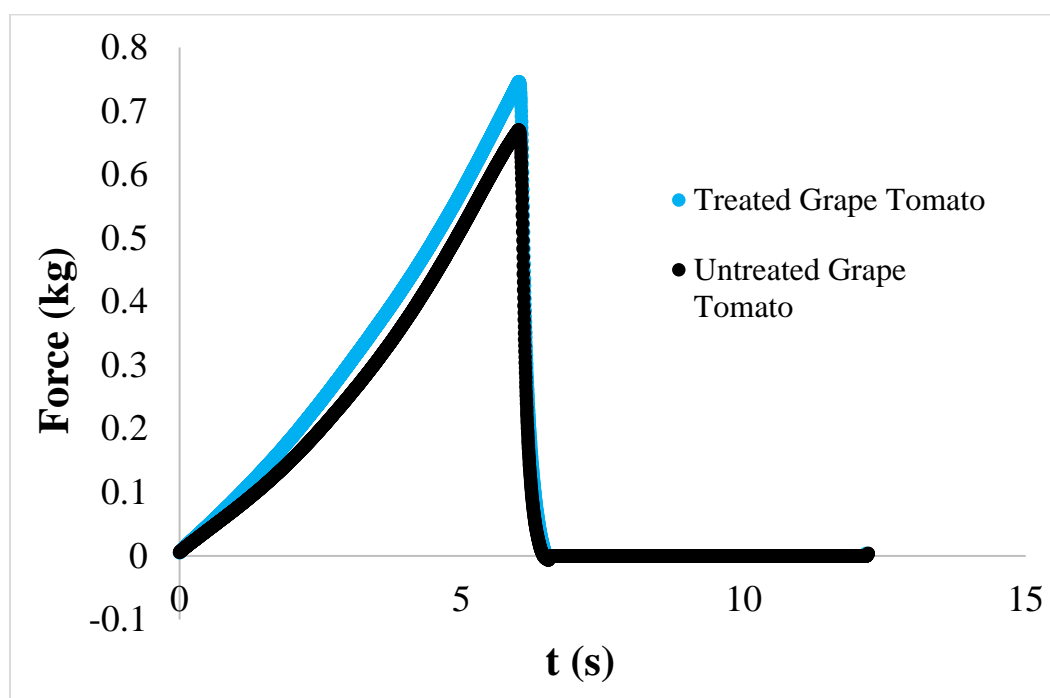


**Figure 8.** Texture profile analysis for treated (2 min., 45 °C, in 9.8 mM octanoic acid) and untreated grape tomatoes.

Similarly, colorimetric analysis data (Table 7) indicate no significant difference at the  $p < 0.05$  level in L ( $t(2) = -1.26$ ,  $p\text{-value} = 0.336$ ), a ( $t(3) = -1.41$ ,  $p\text{-value} = 0.253$ ), and b ( $t(2) = -1.23$ ,  $p\text{-value} = 0.343$ ) values between control and treated grape tomatoes.

**Table 7.** Color parameters for control versus treated (2 min., 45 °C, in 9.8 mM octanoic acid) grape tomatoes

	Control	Treated
L	$10.6 \pm 2.8$	$16.9 \pm 8.4$
a	$14.4 \pm 2.3$	$19.4 \pm 5.7$
b	$10.0 \pm 2.3$	$15.3 \pm 7.0$

Figure 9 illustrates conversion of the average Lab values to RGB ones for untreated and treated grape tomatoes. To the naked eye, the RGB color of untreated versus treated tomato appears nearly identical.

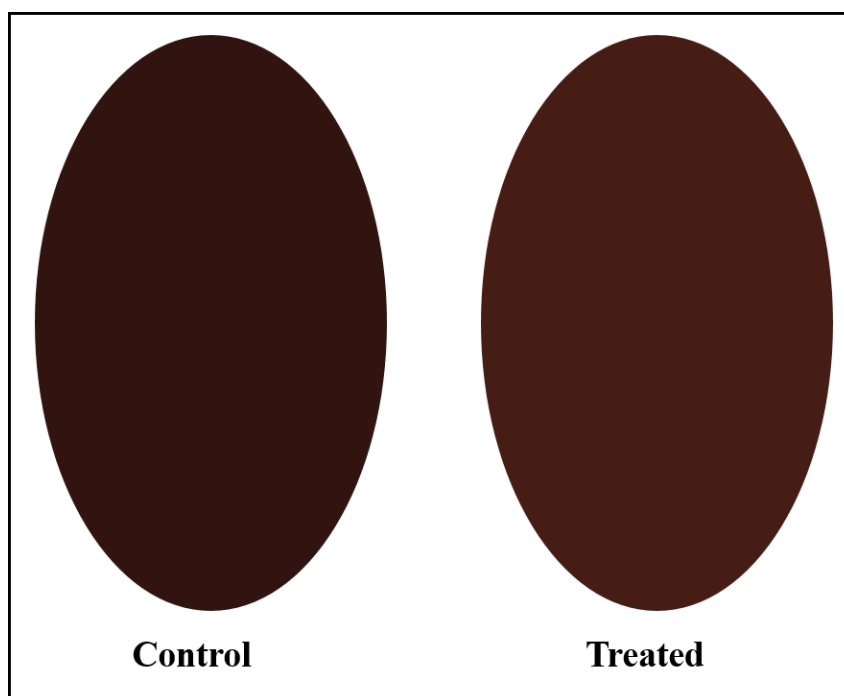


**Figure 9.** RGB values for treated (2 min., 45 °C, in 9.8 mM octanoic acid) and untreated grape tomatoes.

### 3.2.3 Ability of Combined Heat/MCFA to Inhibit Spinach Cross Contamination

Figure 10 strongly suggests that treatment in heated octanoic acid better inhibited cross-contamination of spinach leaves than did treatment with DI water alone (control). Optimal heat/MCFA treatment decreased *E. coli* O157:H7 cross-contamination by ~4 log (10,000-fold) vs. only a ~2 log (100-fold) reduction for DI water treatment.

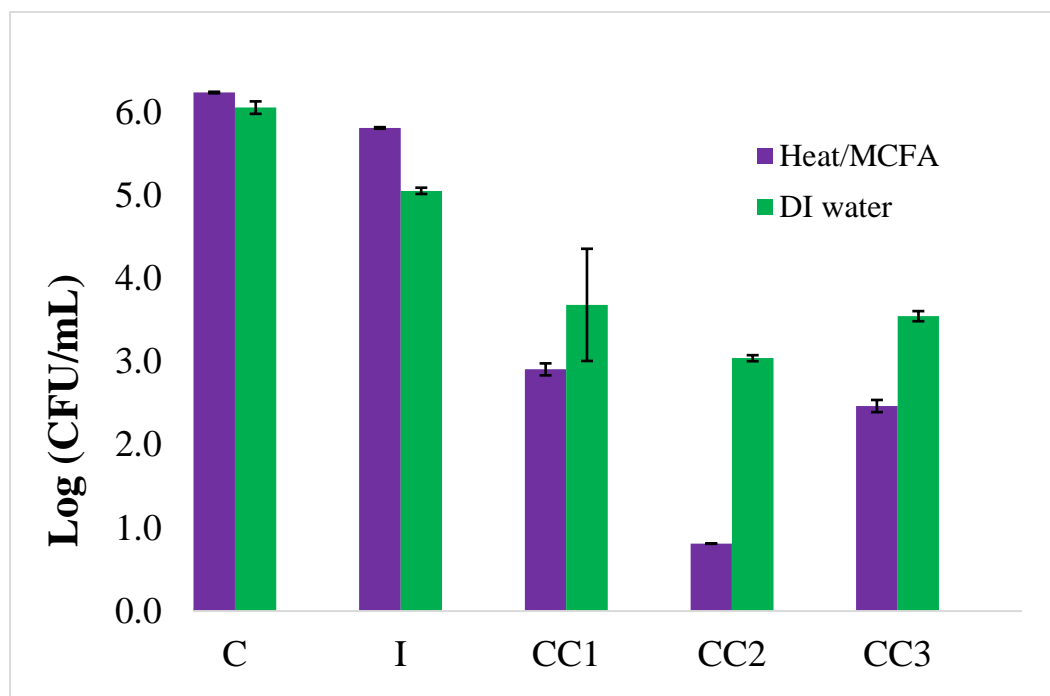


**Figure 10.** Cross-contamination of spinach leaves exposed to *E. coli* O157:H7 after treatment 2 min., 45 °C, in 9.8 mM octanoic acid). C: control leaf; I: inoculated leaf; CC1-CC3: cross contaminated leaves.



## 4. Conclusions and Future Studies

Both low-frequency ultrasound in combination with ZnO and heated medium chain fatty acids show promise as alternative antimicrobial treatments for application to the fresh produce industry.

The quickest and most lethal treatment for *L. innocua* was 8 min. sonication in 40 mM ZnO. Histidine's attenuation of the combined treatment, to a ~1 log reduction, strongly suggests the production of ROS as part of its antibacterial mechanism. The decrease in ZnO nanoparticle size during sonication suggests aggregates of ZnO are being broken apart, making it easier for nanoparticles to penetrate and kill bacteria. Images of *L. innocua* and ZnO particles further imply a physical aspect of ZnO's bactericidal mechanism, as the ZnO particles are associated with bacteria. In addition to ROS generation and physical attachment to bacterial surfaces, ZnO particles may enhance ultrasound's antimicrobial mechanism through other means as well. These may include acting as a nucleation site for generation of more bubbles, and changing the cavitation threshold of bubbles produced by ultrasound. In future studies, these factors need to be investigated further. Experiments must also be done to determine whether application of sonicated ZnO on actual produce (i.e. spinach) affects its quality or appearance.

Based on Box-Behnken trials, optimal conditions for combined heat and medium chain fatty acid treatment were found to be 2 min. at 45 °C in 9.8 mM octanoic acid. Sensory analysis of grape tomatoes subjected to this treatment demonstrated no significant difference in color or texture for these tomatoes in comparison to untreated ones. Further, spinach leaves cross-contaminated with *E. coli* O157:H7 and subsequently

treated with optimal MCFA/heat had on average a 100-fold greater reduction in bacterial contamination than did control (DI water treated) spinach leaves.

For both antimicrobial alternatives, additional studies are required to determine if the treatments are capable of killing other bacteria, such as *E. coli* O157:H7 for sonicated ZnO, *L. innocua* for heated MCFAs, and *Salmonella enterica* spp. for either treatment. If practical studies prove sonicated ZnO effectively removes microorganisms from produce without impairing quality or appearance, ZnO/ultrasound may be a potential alternative to typical chlorine and peroxide based sanitizers where continuous monitoring of solution pH and reagent concentration is required. Since ZnO does not get consumed in the process, it is possible to recycle the solution through multiple cycles of produce washing, thereby saving water and energy. It is also possible to coat food contact surfaces with ZnO that can then be effectively sanitized by exposing them to low-frequency ultrasound. Based on the heated octanoic acid treatments performed on grape tomatoes and spinach, this antimicrobial treatment is a viable option for direct application to fresh produce. Additional studies on different fruits and vegetables are needed to more fully characterize the MCFA/heat treatment's effect on produce quality and ability to inactivate bacteria. Finally, further research is needed to demonstrate the feasibility of either antimicrobial approach at a commercial scale.

## Appendix

### 1. Fluorescein Fluorescence Measurements

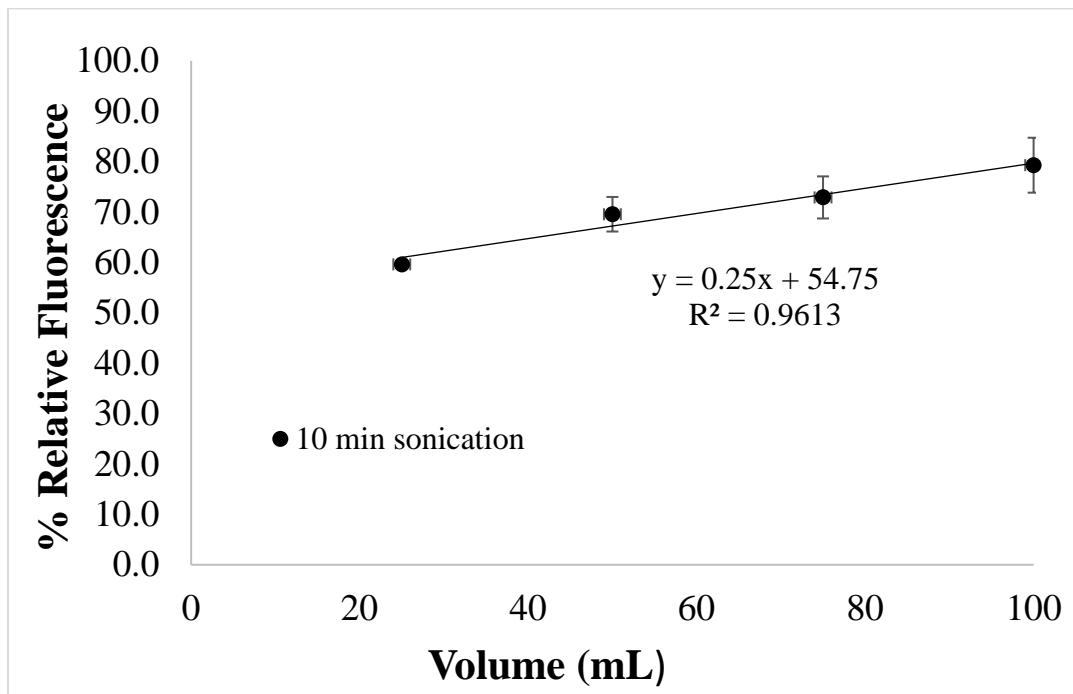
Initially, generation of ROS during sonication of ZnO was assessed by measuring fluorescence of fluorescein, a fluorescent dye which loses its fluorescence upon interaction with ROS. Thus, a decrease in fluorescence or absorbance during sonication would indicate generation of ROS. In the first experiment, fluorescein was added to a final concentration of 5  $\mu\text{M}$  to 25, 50, 75, or 100 mL of 0.1 M phosphate buffer, and sonicated for 10 min. In the second experiment, 5  $\mu\text{M}$  fluorescein in 1 mM ZnO and 0.1 M phosphate buffer was sonicated for 5, 10, 20, and 30 min. In the third, 5  $\mu\text{M}$  fluorescein in 0, 1, or 5 mM ZnO and 0.1 M phosphate buffer was sonicated for 40 min. in 10 min. intervals. The first 10 min. interval was omitted for the 5 mM ZnO trial. Fluorescein fluorescence was measured for all three experiments using a Microplate reader (SpectraMax M5e, Molecular Device Inc., Sunnyvale, CA) at an excitation wavelength of 485 nm and an emission wavelength of 510 nm. Fluorescence values were normalized using the equation:

$$\text{Relative fluorescence intensity} = \frac{100 \times I_t}{I_0}$$

(2)

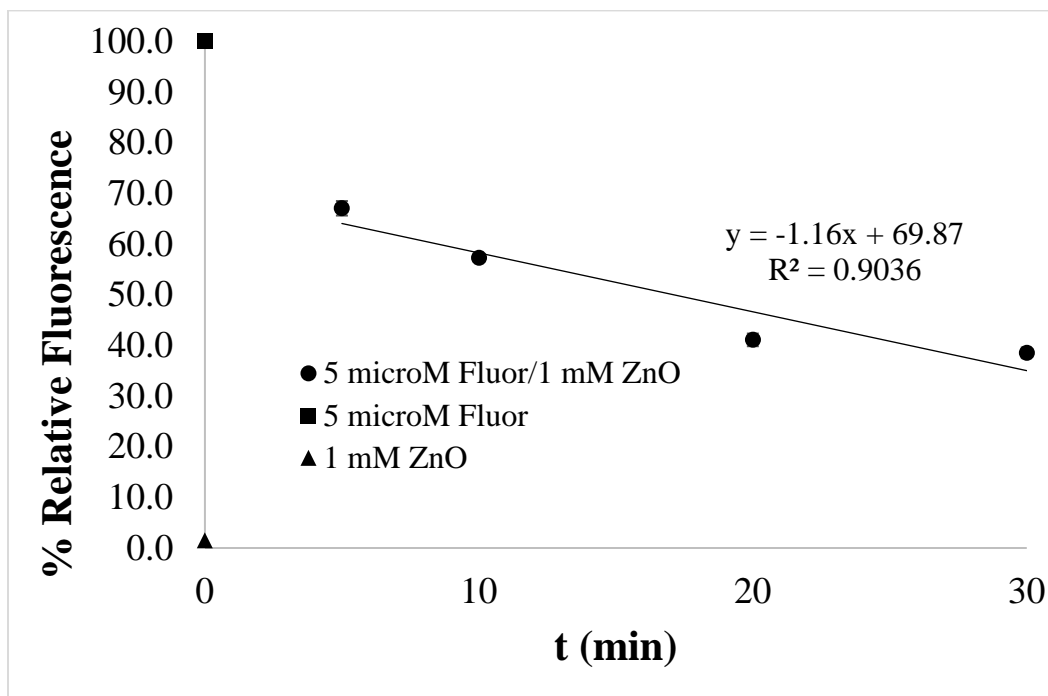
where  $I_0$  is fluorescence intensity at t 0, and  $I_t$  is fluorescence intensity after 't' minutes of sonication.

Results of the first experiment were not meaningful, showing that % relative fluorescence increased with sample volume (Figure 11).



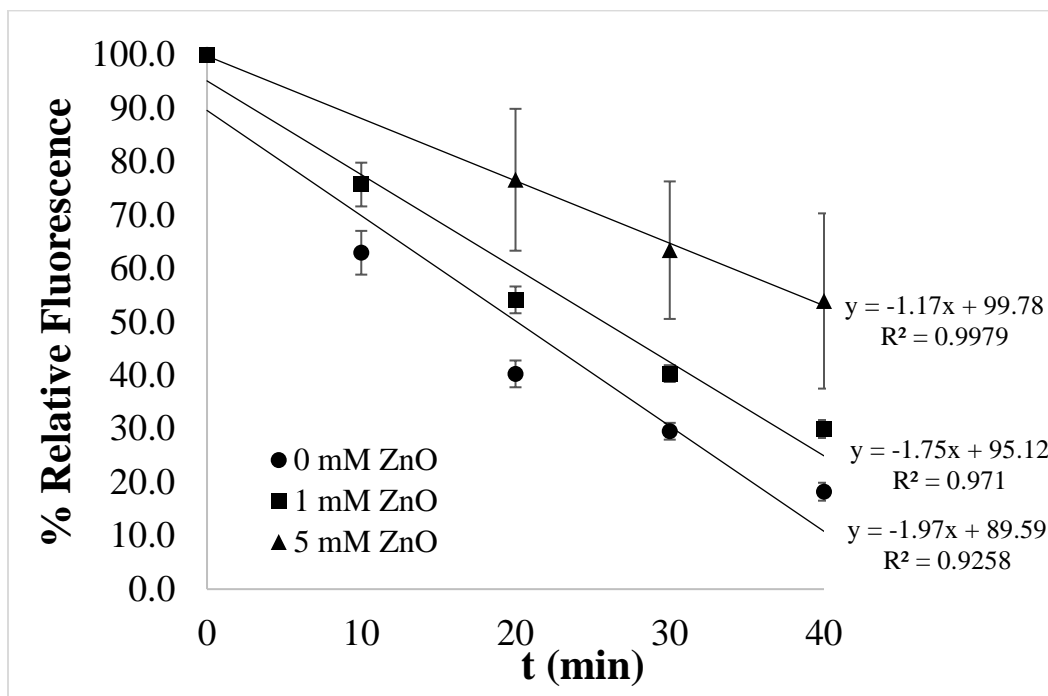
**Figure 11.** Effect of volume sonicated on % relative fluorescence of fluorescein.

Figure 12 shows a decrease in % relative fluorescence with sonication for the second experiment, indicating sonication generates ROS.



**Figure 12.** Effect of combined ZnO and sonication on % relative fluorescence of fluorescein.

The third experiment (Figure 13) demonstrated that with increasing ZnO concentration, decreases in % relative fluorescence lessened. Overall, it was difficult to make any major conclusions based on this data set, other than that sonication likely generates ROS.



**Figure 13.** Effect of increasing concentration of sonicated ZnO on % relative fluorescence of fluorescein.

## 2. Hydrogen Peroxide Detection

### 2.1 Amplex Red Assay

Initial ROS assessments were also done by measuring hydrogen peroxide ( $H_2O_2$ ) generated during sonication. First, an Amplex Red assay, which uses the Amplex Red reagent to detect hydrogen peroxide, was applied to known concentrations of hydrogen peroxide to form a standard curve, as well as to 0.05, 0.1, 0.2, 0.5, and 1 mM ZnO solutions sonicated for 30 min. Second, 50  $\mu$ L of Amplex Red assay containing Amplex Red reagent, horseradish peroxidase, and Dimethyl Sulfoxide, was added to 50  $\mu$ L of each sonicated ZnO solution. These solutions were then covered with aluminum foil to block out light and incubated for 30 min. Finally, absorbance at 560 nm was measured using a Microplate reader.

Figure 14 shows the hydrogen peroxide standard curve, while Figure 15 demonstrates an increase in  $\text{H}_2\text{O}_2$  with an increase in ZnO concentration.

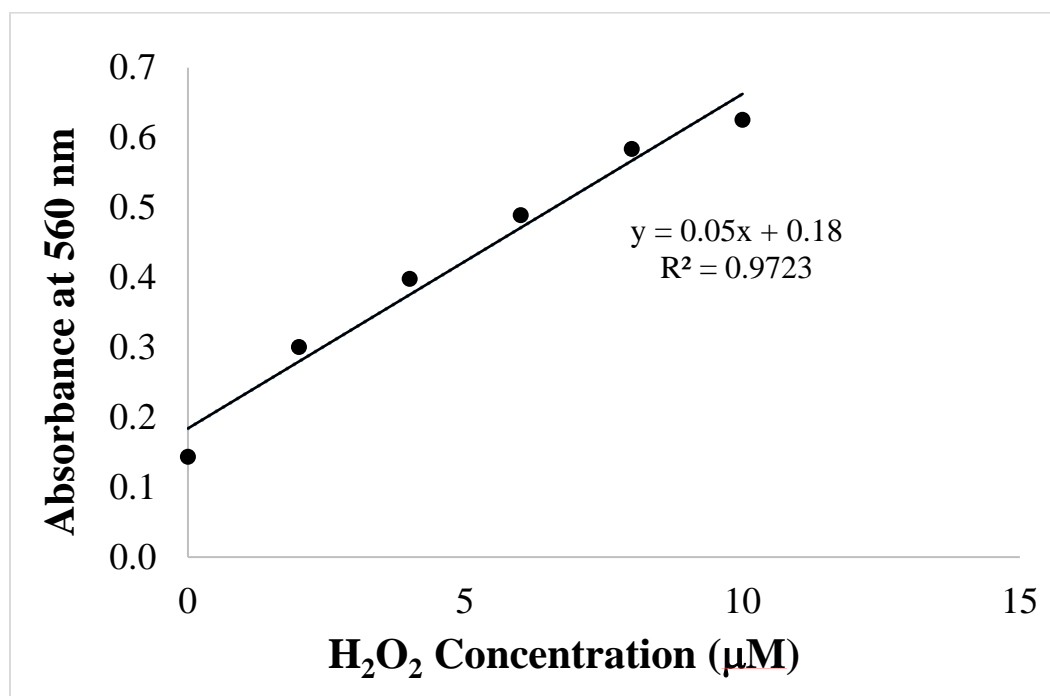


**Figure 14.** Standard curve of hydrogen peroxide measurement by Amplex Red Assay.

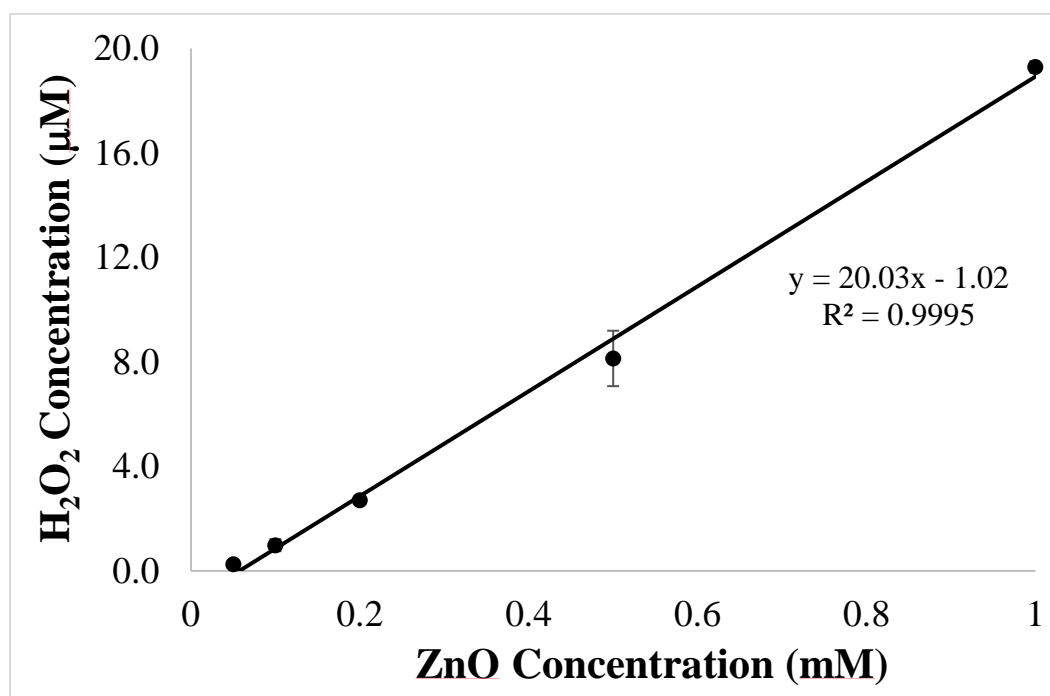


**Figure 15.** Hydrogen peroxide generation upon 30 min. sonication of 0-1 mM ZnO.

## *2.2 Ferrous Ion Oxidation Xylenol Orange Assay*

After an initial Amplex Red Assay experiment, the ferrous ion oxidation xylenol orange (FOX) assay was used because it is much faster. The FOX assay is based on the ability of hydrogen peroxide to convert ferrous ions into ferric ions, which subsequently form a complex with xylenol orange (XO) that can be measured using spectrophotometry. For these experiments, DI water (control) and 40 mM ZnO in DI water were separately sonicated. In the first experiment, 1 mM ZnO and DI water were sonicated 1 hour in 20 min. intervals. In the second one, 4 mM ZnO and DI water were sonicated 1 hour for 20 min. intervals. In the third, 40 mM ZnO and DI water were sonicated 45 min. in 5 min. intervals. After sonication, 300  $\mu$ L of FOX assay (250 mM sulfuric acid, 2.5 mM ferrous sulfate heptahydrate, 1 M sorbitol, and 1 mM xylenol) was added to 100  $\mu$ L of each sonicated DI water and ZnO solution, incubated for 30 min. at room temperature, and absorbance at 560 nm measured using a Microplate reader. Standard curves were prepared for each experiment, but only the standard curve for the first experiment is included (Figure 16).



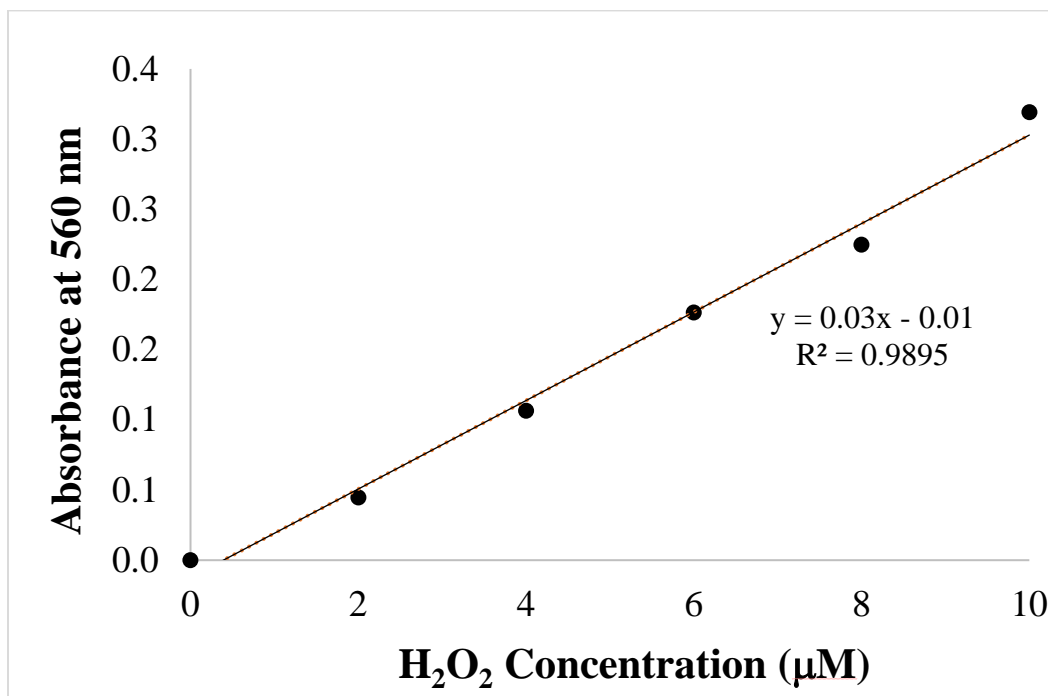


**Figure 16.** Standard curve of hydrogen peroxide concentration by FOX Assay.

Results of the first experiment (Figure 17) suggested a marked increase in H<sub>2</sub>O<sub>2</sub> during sonication in the presence of 1 mM ZnO versus in the absence of ZnO.

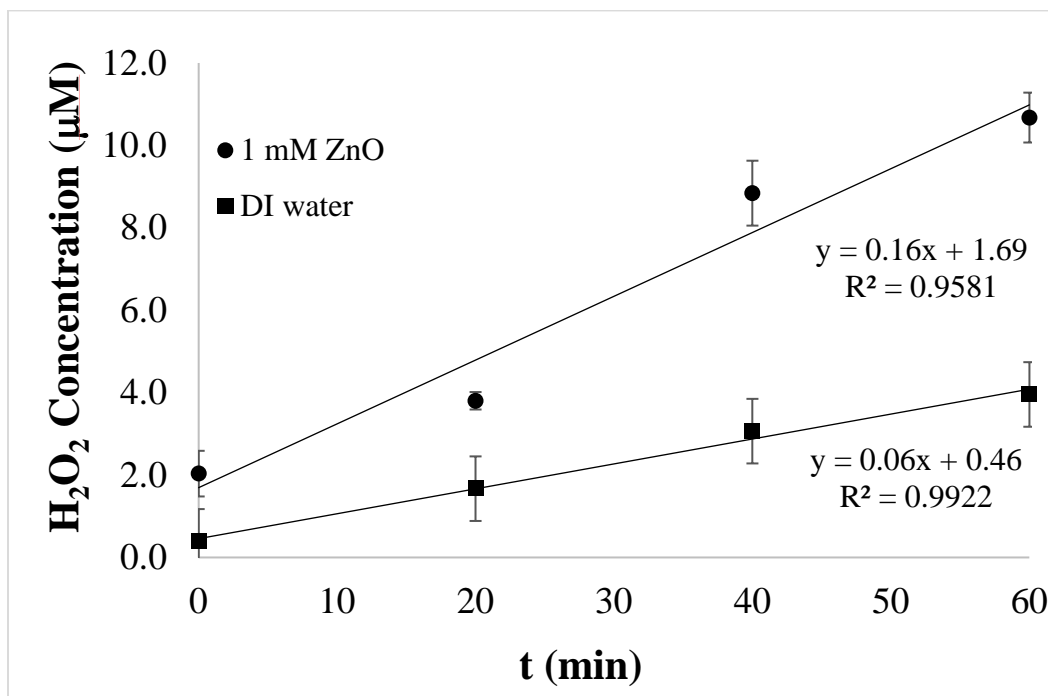


**Figure 17.** Hydrogen peroxide generated in DI water and 1 mM ZnO when sonicated 0-60 min.

However, results of the second experiment (Figure 18) indicated that H<sub>2</sub>O<sub>2</sub> concentration after 60 min. sonication is similar for 4 mM ZnO and DI water.

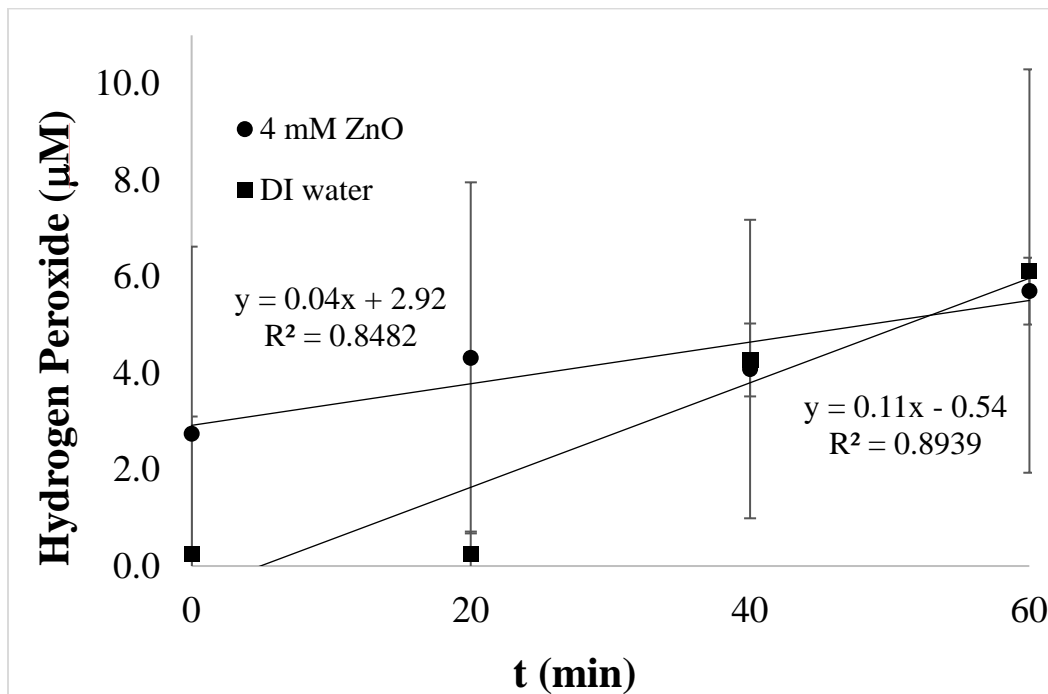


**Figure 18.** Hydrogen peroxide generated in DI water and 4 mM ZnO when sonicated 0-60 min.

Finally, two replicates performed for the third experiment (Figure 19) produced very dissimilar results, suggesting that this is not a viable method for detection of ROS generated via sonication.

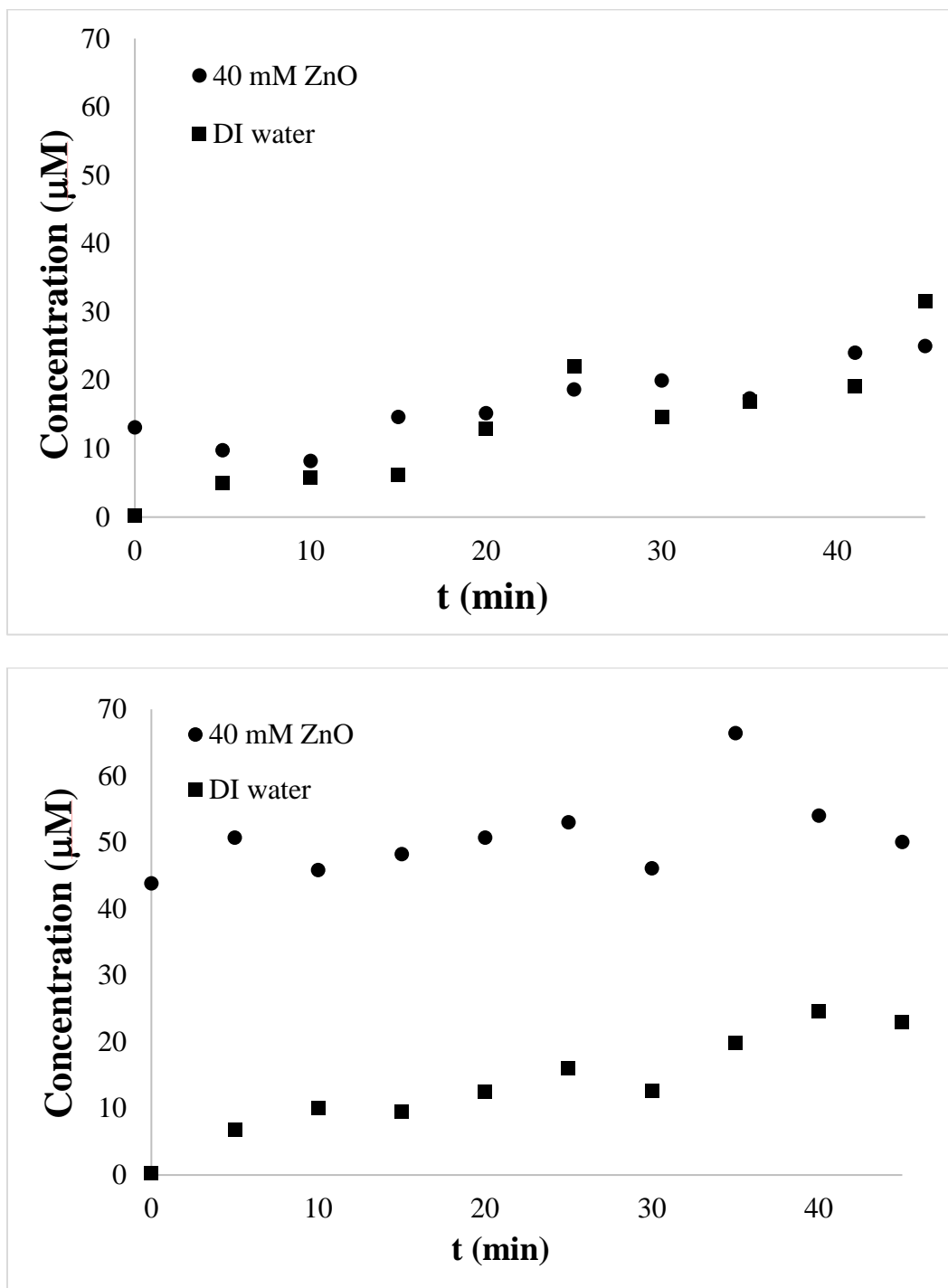


**Figure 19.** Hydrogen peroxide generated in DI water and 40 mM ZnO when sonicated 0-45 min.

## References

Ahvenainen, R., 1996. New approaches in improving the shelf life of minimally processed fruit and vegetables. *Trends Food Sci. Technol*, 7, 179–187.

Ajlouni, S., Sibrani, H., Premier, R., Tomkins, B., 2006. Ultrasonication and fresh produce (*Cos lettuce*) preservation. *J. Food Sci.* 71(2), M62–M68.

AOAC International Official Methods of Analysis. 2009. AOAC International, Gaithersburg, MD.

Artes, F., Gomez, P., Aguayo, E., Escalona, V., Artes-Hernandez, F., 2009. Sustainable sanitation techniques for keeping quality and safety of fresh-cut plant commodities. *Postharvest Biol. Tech.* 51(3), 287–296.

Bermúdez-Aguirre, D., Mobbs, T., Barbosa-Cánovas, G., 2011. Ultrasonic applications in food processing, in: Feng, H., Barbosa-Cánovas, G. (Eds.), *Ultrasound technologies for food and bioprocessing*. Springer, New York, pp. 13-64.

Beuchat, L. R., 1999. Survival of enterohemorrhagic *Escherichia coli* O157:H7 in bovine feces applied to lettuce and the effectiveness of chlorinated water as a disinfectant. *J. Food Protect.*, 62(8), 845-849.

Birmpa, A., Vasiliki, S., Vantarakis, A., 2013. Ultraviolet light and Ultrasound as non-thermal treatments for the inactivation of microorganisms in fresh ready-to-eat foods. *Int. J. Food Microbiol.* 167, 96–102.

Boyette, M. D., Ritchie, D. F., Carballo, S. J., Blankenship, S. M., Sanders, D. C., 1993. Chlorination and postharvest disease control. *HortTechnology*, 3(4), 395–400.

Brayner, R., Ferrari-Iliou, R., Brivois, N., Djediat, S., Benedetti, M. F., Fiévet, F., 2006. Toxicological impact studies based on *Escherichia coli* bacteria in ultrafine ZnO nanoparticles colloidal medium. *Nano Lett.* 6(4), 866–870.

Beuchat, L., Brackett, R., 1990. Survival and growth of *Listeria monocytogenes* on lettuce as influenced by shredding, chlorine treatment, modified atmosphere packaging, and temperature. *J. Food Sci.* 55 , 755–775.

Boyaval, P., Corre, C., Dupuis, C., Roussel, E., 1995. Effects of free fatty acids on propionic acid bacteria. *Lait.* 75:17–29.

Casolari, A., 1988. Microbial death. In: Bazin, M.J., Prosser, J.I., editors. *Physiological Models in Microbiology*, vol. II. Boca Raton: CRC Press. p.1–44.

CDC, 2016. List of selected multistate foodborne outbreak investigations.

CSPI, 2015. Outbreak alert! 2015; a review of foodborne illness in the U.S. from 2004 – 2013.

Erriu, M., Blus, C., Szmukler-moncler, S., Buogo, S., Levi, R., Barbato, G., Orrù, G., 2014. Microbial biofilm modulation by ultrasound: current concepts and controversies. *Ultrasonics – Sonochemistry* 21(1), 15–22.

Desbois, A. P., Smith, V. J., 2010. Antibacterial free fatty acids: Activities, mechanisms of action and biotechnological potential. *Applied Microbiol. Biotechnol.*, 85(6), 1629–1642.

Emami-Karvani, Z., Chehrazi, P., 2011. Antibacterial activity of ZnO nanoparticle on gram-positive and gram-negative bacteria. *Afr. J. Microbiol. Res.* 5(12), 1368–1373.

Dickson, J. S., 1992. Acetic acid action on beef tissue surfaces contaminated with *Salmonella typhimurium*. *J. Food Sci.* 57:297–301.

Espitia, P. J. P., Soares, N. D. F. F., Coimbra, J. S. D. R., de Andrade, N. J., Cruz, R. S., Medeiros, E. A. A., 2012. Zinc oxide nanoparticles: synthesis, antimicrobial activity and food packaging applications. *Food Bioprocess Technol.* 5(5), 1447–1464.

FDA, 2001. Outbreaks associated with fresh and fresh-cut produce. Incidence, growth, and survival of pathogens in fresh and fresh-cut produce. In: Analysis and evaluation of preventive control measures for the control and reduction/elimination of microbial hazards on fresh and fresh-cut produce executive summary.

FDA, 2015. Preventive control measures for fresh and fresh-cut produce.

FDA, 2016. 21CFR172.860: Food additives permitted for direct addition to food for human consumption; fatty acids.

Ferrante, S., Guerrero, S., Alzamora, S. M., 2016. Combined use of ultrasound and natural antimicrobials to inactivate *Listeria monocytogenes* in orange juice. *J. Food Protect.* 70, 1850–1856.

Friedly, E. C., Crandall, P. G., Ricke, S., O'Bryan, C. A., Martin, E. M., Boyd, L. M., 2008. Identification of *Listeria innocua* surrogates for *Listeria monocytogenes* in hamburger patties. *J. Food Sci.*,73(4), 174–178.

Galbraith, H., Miller, T. B., 1973. Effect of long chain fatty acids on bacterial respiration and amino acid uptake. *J. Appl. Bacteriol.* 36:659–675.

Georgel, P., Crozat, K., Lauth, X., Makrantonaki, E., Seltmann, H., Sovath, S., Hoebe, K., Du, X., Rutschmann, S., Jiang, Z., Bigby, T., Nizet, V., Zouboulis, C.C., Beutler, B., 2005. A toll-like receptor 2-responsive lipid effector pathway protects mammals against skin infections with Gram-positive bacteria. *Infect Immun* 73:4512–4521.



Gil, M. I., Selma, M. V, López-gálvez, F., & Allende, A., 2009. Fresh-cut product sanitation and wash water disinfection: problems and solutions. *Int. J. Food Microbiol.* 134(1-2), 37–45.

Gurtler, J. B., Rivera, R. B., Zhang, H. Q., Gevecke, D. J., 2010. Selection of surrogate bacteria in place of *E. coli* O157:H7 and *Salmonella* Typhimurium for pulsed electric field treatment of orange juice. *Int. J. Food Microbiol.*, 139(1-2), 1–8.

Hassinen, J.B., Durbin, G.T., Bernhart, F.W., 1951. The bacteriostatic effect of saturated fatty acids. *Arch. Biochem. Biophys.* 31: 183–189.

Jalal, R., Goharshadi, E.K., Abareshi, M., Moosavi, M., Yousefi, A., Nancarrow, P., 2010. ZnO nanofluids: green synthesis, characterization, and antibacterial activity. *Mater. Chem. Phys.* 121(1), 198–201.

Jang, H. I., Rhee, M. S., 2009. Inhibitory effect of caprylic acid and mild heat on *Cronobacter* spp. (*Enterobacter sakazakii*) in reconstituted infant formula and determination of injury by flow cytometry. *Int. J. Food Microbiol.* 133(1-2), 113–120.

Jin, T., Sun, D., Su, J. Y., Zhang, H., Sue, H. J., 2009. Antimicrobial efficacy of zinc oxide quantum dots against *Listeria monocytogenes*, *Salmonella* Enteritidis, and *Escherichia coli* O157:H7. *J. Food Sci.* 74(1), M46-M52.

Johnson, L. L., Peterson, R. V., Pitt, W. G., 2016. Treatment of bacterial biofilms on polymeric biomaterials using antibiotics and ultrasound. *J. Biomater. Sci. Polym. Ed.* 9(11), 1177-1185.

Jones, N., Ray, B., Ranjit, K.T., Manna, A.C., 2008. Antibacterial activity of ZnO nanoparticles suspensions on a broad spectrum of microorganisms. *FEMS Microbiol. Lett.* 279(1), 71-76.

Kenny, J.G., Ward, D., Josefsson, E., Jonsson, I.-M., Hinds, J., Rees, H. H., Lindsay, J.A., Tarkowski, A., Horsburgh, M.J., 2009. The *Staphylococcus aureus* response to unsaturated long chain free fatty acids: survival mechanisms and virulence implications. *PLoS One* 4: e4344.

Kihm, D., Leyer, G., An, G., Johnson, E., 1994. Sensitization of heat-treated *listeria monocytogenes* to added lysozyme in milk. *Appl. Environ. Microbiol.* 60(10), 3854 – 3861.

Kim, J. K., Harrison, M. A., 2009. Surrogate selection for *Escherichia coli* O157:H7 based on cryotolerance and attachment to romaine lettuce. *J. Food Protect.* 72(7), 1385–1391.

Kuldiloke, J., 2002. Effect of ultrasound, temperature and pressure treatments on enzyme activity and quality indicators of fruit and vegetable juices. PhD dissertation.

Lawton, M., Kinchla, A. 2015. Produce wash water sanitizers: chlorine and PAA. UMass Amherst Extension: Vegetable Program. Available from:

<https://ag.umass.edu/vegetable/fact-sheets/produce-wash-water-sanitizers-chlorine-paa>.

Accessed March 27, 2017.

Li, Y., Brackett, R. E., Chen, J., Beuchat, L. R., 2001. Survival and growth of *Escherichia coli* O157:H7 inoculated onto cut lettuce before or after heating in chlorinated water , followed by storage at 5 or 15 degrees C. *J. Food Protect.* 64(3):305-9.

Liaw, S.-J., Lai, H.-C., Wang, W.-B. , 2004. Modulation of swarming and virulence by fatty acids through the *rsbA* protein in *Proteus mirabilis*. *Infect. Immun.* 72:6836–6845.

Lipovsky, A., Nitzan, Y., Gedanken, A., Lubart, R., 2011. Antifungal activity of ZnO nanoparticles — the role of ROS mediated cell injury. *Nanotechnology.* 22(10).

Mañas, P., Pagán, R., Raso, J., Sala, F. J., Condón, S., 2000. Inactivation of *Salmonella enteritidis*, *Salmonella typhimurium*, and *Salmonella senftenberg* by ultrasonic waves under pressure. *J. Food Prot.* 63(4), 451–456.

Marounek, M., Putthana, V., Benada, O., & Lukešová, D., 2012. Antimicrobial activities of medium-chain fatty acids and monoacylglycerols on *Cronobacter sakazakii* DBM 3157T and *Cronobacter malonaticus* DBM 3148. *CJFS*, 30(6), 573–580.

Miller, R. D., Brown, K. E., Morse, S. A., 1977. Inhibitory action of fatty acids on the growth of *Neisseria gonorrhoeae*. *Infect. Immun.* 17:303–312.

Murphy, R. Y., Beard, B. L., Martin, E. M., Keener, A. E., Osaili, T., 2004. Predicting process lethality of *Escherichia coli* O157:H7, *Salmonella*, and *Listeria monocytogenes* in ground, formulated, and formed beef/turkey links cooked in an air impingement oven. *Food Microbiol.* 21(5): 493-499.

Mvou, B., Coroller, L., Mathot, A.G., Mafart, P., Leguerinel, I., 2010. Modelling the influence of palmitic, palmitoleic, stearic and oleic acids on apparent heat resistance of spores of *Bacillus cereus* NTCC 11145 and *Clostridium Sporogenes* Pasteur 79.3.

Ordoñez, J. A, Aguilera, M. a, Garcia, M. L., & Sanz, B., 1987. Effect of combined ultrasonic and heat treatment (thermoultrasonication) on the survival of a strain of *Staphylococcus aureus*. *J. Dairy Res.* 54, 61–67.

Painter, J. A., Hoekstra, R. M., Ayers, T., Tauxe, R. V, Braden, C. R., Angulo, F. J., Griffin, P. M., 2013. Attribution of Foodborne Illnesses, Hospitalizations, and Deaths to

Food Commodities by using Outbreak Data, United States, 1998-2008. *Emerg. Infect. Diseases* 19(3), 407–415.

Padmavathy, N., Vijayaraghavan, R., 2008. Enhanced bioactivity of ZnO nanoparticles— an antimicrobial study. *Sci. Technol. Adv. Mater.* 9(3), 035004.

Paster, N., 1979. A commercial scale study of the efficiency of propionic acid and calcium propionate as fungistats in poultry feed. *Poult. Sci.* 58:572–576.

Piyasena, P., Mohareb, E., Mckellar, R. C., 2003. Inactivation of microbes using ultrasound : a review. *Int. J. of Food Microbiol.* 87, 207–216.

Raghupathi, K.R., Koodali, R.T., Manna, A.C., 2011. Size-dependent bacterial growth inhibition and mechanism of antibacterial activity of zinc oxide nanoparticles. *Langmuir* 27(7), 4020–4028.

Rico, D., Martín-Diana, A. B., Barat, J. M., Barry-Ryan, C., 2007. Extending and measuring the quality of fresh-cut fruit and vegetables: a review. *Trends Food Sci. Technol.* 18(7), 373–386.

Sala, F. J., Burgos, J., Cóndon, S., Lopez, P., Raso, J. (1995). Effect of heat and ultrasound on microorganisms and enzymes. In G.W. Gould (Ed.), *New methods of food preservation* (pp. 176-204). London: Chapman and Hall.

Sawai J., Shoji, S., Igarashi, H., Hashimoto, A., Kokugan, T., Shimizu, M., Kojima, H., 1998. Hydrogen peroxide as an antibacterial factor in zinc oxide powder slurry. J. Ferment Bioeng. 86:521–2.

Scherba, G., Weigel, R. M., & Brien, W. D. O., 1991. Quantitative Assessment of the Germicidal Efficacy of Ultrasonic Energy. *Appl. Environ. Microbiol.* 57(7), 2079–2084.

Scouten, A. J., Beuchat, L. R., 2002. Combined effects of chemical, heat and ultrasound treatments to kill *Salmonella* and *Escherichia coli* O157:H7 on alfalfa seeds. *J. Appl. Microbiol.* 92(4), 668–674.

Seil, J.T., Webster, T.J., 2012. Antibacterial effect of zinc oxide nanoparticles combined with ultrasound. *Nanotechnology.* 23(49).

Sharma, M., Adler, B. B., Harrison, M. D., Beuchat, L. R., 2005. Thermal tolerance of acid-adapted and unadapted *Salmonella*, *Escherichia coli* O157:H7, and *Listeria monocytogenes* in cantaloupe juice and watermelon juice. *Lett. Appl. Microbiol.*, 41(6), 448–453.

Sheu, C. W., Freese, E., 1972. Effects of fatty acids on growth and envelope proteins of *Bacillus subtilis*. *J. Bacteriol.* 111:516–524.

Shimizu, M. (1998). Factor in Zinc Oxide, 86(5), 521–522.

Sousa, C., Sequeira, D., Kolen, Y., Pinto, I., Petrovykh, D., 2015. Analytical protocols for separation and electron microscopy of nanoparticles interacting with bacterial cells. *Anal. Chem.* 87(9), 4641 – 4648.

Takigawa, H., Nakagawa, H., Kuzukawa, M., Mori, H., Imokawa, G. 2005. Deficient production of hexadecenoic acid in the skin is associated in part with the vulnerability of atopic dermatitis patients to colonisation by *Staphylococcus aureus*. *Dermatology* 211:240–248.

Thormar, H., Hilmarsson, H., Bergsson, G., 2006. Stable concentrated emulsion of the 1-monoglyceride of capric acid (monocaprin) with microbicidal activities against the food-borne bacteria *Campylobacter jejuni*, *Salmonella* spp., and *Escherichia coli*. *Appl. Environ. Microbiol.* 72: 522–526.

Tsuchido, T., Takano, M., 1988. Sensitization by heat treatment of *Escherichia coli* K-12 cells to hydrophobic antibacterial compounds. *Antimicrob. Agents Chemother.* 32(11), 1680–1683.

Van Immerseel, F., De Buck, J., Boyen, F., Bohez, L., Pasmans, F., Volf, J., Sevcik, M., Rychlik, I., Haesebrouck, F., Ducatelle, R., 2004. Medium-chain fatty acids decrease colonization and invasion of chickens with *Salmonella enterica* serovar enteritidis. *Appl. Environ. Microbiol.* 70: 3582–3587.

Villamiel, M., Gamboa, J., Soria, A. C., Riera, E., García-, J. V, & Montilla, A., 2015. Impact of power ultrasound on the quality of fruits and vegetables during dehydration. *Phys. Procedia.* 70: 828–832.

Wahab, R., Mishra, A., Yun, S., Kim, Y. S., Shin, H. S., 2010. Antibacterial activity of ZnO nanoparticles prepared via non-hydrolytic solution route. *Appl. Microbiol. Biotechnol.* 87(5), 1917–1925.

Wojtczak, L., Więckowski, M. R., 1999. The mechanisms of fatty acid induced proton permeability of the inner mitochondrial membrane. *J. Bioenerg. Biomembr.* 31:447–455.

Xiong, R., Xie, G., Edmondson, A. E., Sheard, M. A., 1999. A mathematical model for bacterial inactivation. *Int. J. Food Microbiol.* 46, 45–55.

Zhang, S., Farber, J.M., 1996. The effects of various disinfectants against *Listeria monocytogenes* on fresh-cut vegetables. *Food Microbiol.*, 13(4), 311–321.



Zhang, L., Jiang, Y., Ding, Y., Povey, M., York, D., 2007. Investigation into the antibacterial behaviour of suspensions of ZnO nanoparticles (ZnO nanofluids). *J. Nanopart. Res.* 9(3), 479–489.